Slotted Substrate Integrated Waveguide Array Antenna & Feed System

Bronte MacIntosh-Hobson

A Thesis

in

The Department

of

Electrical and Computer Engineering

Presented in Partial Fulfillment of the Requirements
for the Degree of Master of Applied Science (Electrical Engineering) at
Concordia University
Montreal, Quebec, Canada

August 2008

Your file Votre référence
ISBN: 978-0-494-45491-6
Our file Notre référence
ISBN: 978-0-494-45491-6

ABSTRACT

Slotted Substrate Integrated Waveguide Array Antenna & Feed System

Bronte MacIntosh-Hobson

In this thesis we investigate substrate integrated waveguides and their application as a slotted waveguide antenna array. The standard slotted waveguide antenna is designed following Elliot's modified design procedure. Elliot's modified design procedure not only takes into account the effects of mutual coupling from the neighboring slots in the array but also the internal higher order modes that are scattered off adjacent slots. The antenna is then converted to a slotted substrate integrated waveguide antenna by carefully placing two rows of metallic via holes to simulate the sidewalls of the rectangular waveguide. The size and location of the via holes are calculated such that they contain the electromagnetic fields inside the substrate integrated waveguide with negligible leakage loss and that the substrate integrated waveguide has the same propagation constant and characteristic impedance as its equivalent rectangular waveguide. Integrating the waveguide into a substrate allows the entire circuit to be fabricated within the substrate and eliminates the need for complicated transitions that link a rectangular waveguide to a planar circuit. The antenna is fed by a 50Ω shielded stripline. The stripline is shielded by two rows of via holes placed symmetrically on each side of the trace of the stripline. The transition is composed of a single via hole that links the shielded stripline to the substrate integrated waveguide. Back-to-back transitions between a shielded stripline and a substrate integrated waveguide are designed and simulated for three different frequency bands; C band, Ku band & Ka band. The bandwidth of the transitions ranged from 20-35% in all cases. A back-to-back transition was fabricated for the C-band. The fabrication

was done by hand using electrical tape for the stripline inner conductor and screws as the via holes. The bandwidth of the measured results show a smaller bandwidth compared to the simulated results. This disparity is due to the imperfections associated with fabricating the transition by hand. A uniform antenna array of 8 slots is designed and simulated with the feed network. A good radiation pattern with sidelobes 14dB below the main beam is observed. The antenna has an impedance bandwidth of 1GHz at the operating frequency of 15GHz.

Acknowledgements

I would like to thank my supervisor Dr. Sebak whose insightful guidance and helpful and open demeanor allowed me to complete this thesis. I would also like to thank my colleague Mike Wong for his support and knowledgeable discussions which helped me write this thesis.

Table of Contents

List of Symbols

θ.....Theta, angle

ε.....Epsilon, permittivity

δ.....Delta, loss tangent

γ.....Gamma, propagation constant

β.....Beta, imaginary part of propagation constant

α.....Alpha, real part of propagation constant

η.....Eta, characteristic impedance of free-space

ζ.....Zeta, variable

λ.....Lamda, wavelength

μ.....Mew, permeability

φ.....Phi, angle

π.....Pi

s.....via hole spacing

d.....via hole diameter

a.....substrate integrated waveguide width

b.....substrate integrated waveguide height

a_{RWG}.....waveguide width

f.....frequency

k.....wavenumber

A.....forward-scattered amplitude

B.....backward-scattered amplitude

E.....electric field

H.....magnetic field

x.....offset

V_s.....slot voltage

l.....slot length

l_r.....slot resonant length

z.....propagation distance

Y_n.....active admittance

V_n.....mode voltage

G_0.....waveguide characteristic conductance

g_{mn}.....mutual coupling

R.....local variable adjacent slot distance

P.....local variable location inside slot

h_n.....higher order mode coupling

MC_n.....mutual coupling term

g.....rectangular coax parameter

h.....rectangular coax parameter

C_{fl}.....rectangular coax parameter

Zi.....input impedance

$(Z_0)_{01}$.....waveguide impedance

S_c.....short circuit distance

R_{leak}.....substrate integrated waveguide leakage

k_c.....cutoff frequency wavenumber

c_0.....speed of light

β_{siw}.....substrate integrated waveguide propagation constant

L_1, L_2.....substrate integrated waveguide section length

w.....slot width

G.....conductance

G_r.....resonant conductance

f_c.....cutoff frequency

$\angle S_{21}^{L1}$ .....phase shift

List of Abbreviated Terms

SIW.....Substrate Integrated Waveguide

SIRC.....Substrate Integrated Rectangular Coaxial

MoM.....Method of Moments

BI-RME.....Boundary Integral-Resonant Mode Expansion

RWG.....Rectangular Waveguide

GCPW.....Grounded Co-Planar Waveguide

ABC.....Absorbing Boundary Condition

List of Figures

List of Tables

Chapter 1

Introduction

1.1 Introduction

The slotted waveguide antenna is a type of aperture antenna. It can provide a large gain and has high power handling capabilities and finds many applications in radar and communication systems. The physical structure of a waveguide is large and bulky and it requires complicated transitions for connection with planar circuitry. Rectangular waveguides and the transitions needed to integrate them with planar circuitry are expensive and voluminous. Substrate integrated waveguides (SIWs) are a relatively new type of planar transmission line which essentially integrate a waveguide into a planar circuit such as a printed circuit board or a low-temperature co-fired ceramic. Substrate integrated waveguides incorporate the advantages of rectangular waveguides, such as high power handling capacity, high Q-factor and low loss, into planar circuitry [1]. In addition SIWs allow for easy transition between other planar transmission lines and they are small, have a low-profile and weigh less compared to rectangular waveguides.

1.2 Problem Statement

This thesis focuses on the integration of a slotted waveguide antenna into a planar circuit using substrate integrate waveguide theory. A vertical transition is presented that allows the slotted substrate integrated waveguide antenna to be fed by a simple stripline, with the requirement that the transition's bandwidth is larger than the antenna's bandwidth.

1.3 Motivation & Applications

The slotted waveguide antenna is an aperture antenna. Large arrays can be formed with this type of antenna. Figure 1.1 shows a picture of a slotted waveguide antenna.

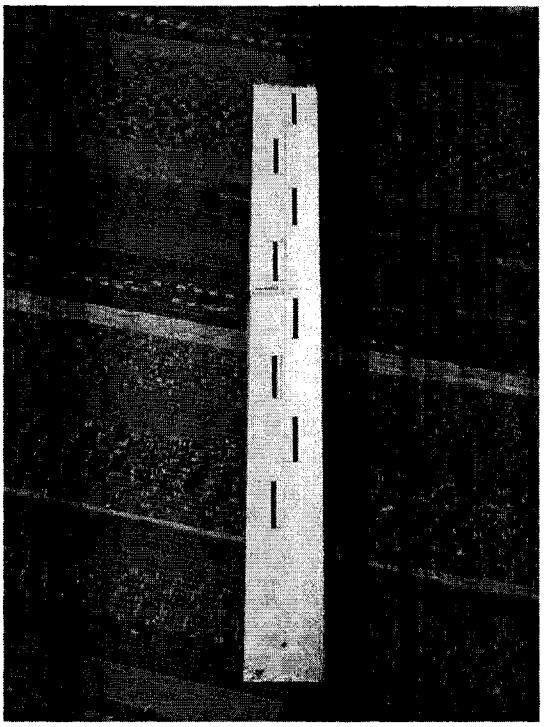

Figure 1.1: Picture of a slotted waveguide antenna [2].

This property allows designers to design slotted waveguide antennas with a large amount of gain and correspondingly a very narrow beamwidth. A waveguide itself is very robust and durable and has a high power handling capacity. Due to the antennas geometry it can be mounted flush on the fuselage of an airplane. These qualities find the slotted waveguide antenna used in numerous applications. The slotted waveguide antenna is especially well fitted for radar applications thanks to its large gain and small beamwidth. Unfortunately waveguides are large bulky, heavy objects. They cannot be easily integrated with other microwave circuitry. Expensive transitions must be designed and

built in order to connect the waveguide to the rest of the microwave circuit [3-6]. This thesis is concerned with taking a slotted waveguide antenna and integrating it directly into the substrate. This thesis also develops a feeding scheme that allows the integrated antenna to be fed through a basic microwave transmission line, the stripline. There are some definite advantages to integrating a slotted waveguide antenna directly into the substrate. First of all, the transitions between a waveguide and a planar circuit are no longer needed. These transitions must be carefully built and are very difficult to mass produce. The transition proposed in this thesis is simple enough to build and allows the antenna to easily communicate with the rest of the microwave circuit. Since the antenna and its feeding scheme are entirely contained within the substrate, the circuit can be reliably mass manufactured, significantly reducing the cost of the circuit. In the industry being able to mass manufacture a circuit is an indispensable design goal. Having the waveguide integrated into the substrate allows the overall circuit to have a smooth low-profile appearance.

1.4 Objectives & Problems

In this thesis we are faced with two main objectives: (1) the design of a linear substrate integrated slotted waveguide antenna with longitudinal slots and (2) the design of a vertical transition between a microwave stripline and a substrate integrated waveguide. The SIW antenna is fed by a stripline, which is a common type of microwave transmission line. When designing the antenna itself, a modified Elliot's procedure [7,8,9] is used which takes higher order mode coupling into account. Elliot's procedure [7,8,9] is originally for rectangular waveguides, but the procedure can used successfully

for slotted SIW antennas. The two main differences between each type of waveguide are: (1) the sidewalls of the SIW are made up of carefully placed via holes and (2) the thickness of the SIW is considerably smaller compared to regular bulky waveguides. The designer must be aware of how changes in waveguide thickness, dimension *b*, have an affect on the interactions between the electromagnetic fields and the longitudinal slots and how they affect the overall performance of the antenna. In multi-layered microwave circuits different types of transmission lines are used for different applications. One of the most popular and abundantly used transmission lines is the microstrip line. For this reason we also present the design of a transition between a microstrip line and a stripline line. This allows the input signal coming from a microstrip line to be fed into the SIW antenna.

1.5 Basic Assumptions & Limitations

The design of the whole antenna system is limited by the fabrication technology. The circuit is limited to two double-sided substrate layers and because of the via hole metallization procedure it can be no larger than 4"X4"[10]. This puts a limit on the size of the SIW and thus the amount of slots we can use for the antenna. There are also strict limits upon the via hole diameter relative to the substrate thickness as well as the spacing between adjacent vias. The maximum substrate thickness we can use is 60mil. Since the proposed circuit is a double layered PCB each individual thickness is limited to 30mil. The thickness of the circuit sets the limit on the minimum via hole diameter. The diameter to height ratio must be greater than one; $D/H > 1$ [10]. This constricts the via holes to have a diameter no smaller than 60mil. When fabricating multi-layered circuits it

is wise to choose a substrate that works well with the adhesive used to glue the substrates together. For this reason the substrate is chosen to be Rogers Duroid 6002 with a dielectric permittivity of ε_r=2.94 and a loss tangent of δ=0.0012.

1.6 Document Overview

Chapter 2 gives a review of the literature which is related to this thesis. The chapter begins with previous work on the design of a slotted waveguide antenna and the improvements on design procedure are discussed. Works on substrate integrated waveguides and how their characteristics are extracted are presented. Work on slotted substrate integrated waveguide antennas are mentioned with some results listed. Previous work concerning transitions between microstrip lines and SIW are discussed in chapter 2. The theory relating to this thesis is discussed in chapter 3. The chapter begins with a discussion on the characteristics of a slot cut out of the broad wall of a rectangular waveguide. Design equations describing the electric field induced in a slot are shown. A design procedure for a slotted waveguide making use of the slot voltage equations is described. The second half of the chapter discusses the antenna fed structure. The feeding scheme comprises of a shielded stripline and a vertical transition between the stripline and SIW. The geometry and theory of the transition is discussed. Chapter 3 also discusses the theory and methodology of transforming a rectangular waveguide into a substrate integrated waveguide.

Chapter 4 presents the results of different components of the antenna and its feeding structure. It begins with the self-admittance characterization of a single slot. This data is then used to design a slotted waveguide antenna, the results of the S-parameters and

radiation pattern of the antenna is given in chapter 4. A rectangular waveguide and its equivalent SIW are simulated together to see how well they match. The same is done for a rectangular coax line and a shielded stripline. Chapter 4 also discusses the results of the vertical transition between the shielded stripline and SIW over different frequency bands. The chapter concludes with a discussion of the simulation results of the entire antenna including its feeding scheme.

Chapter 5 gives a conclusion to the thesis. It also discusses future work on the subject of SIW and microwave transitions.

Chapter 2

Literature Review

2.1 Introduction

Previous research related to slotted waveguide antennas, substrate integrated waveguides, substrate integrated waveguide antennas and transitions between microwave transmission lines and substrate integrated waveguides are discussed in this chapter. Beginning the discussion with Elliot's procedure [7,8,9] for designing slotted waveguide antennas then move on to work by Wu & Deslandes [1,4,5] on SIWs and how they can be designed to mimic rectangular waveguides. The chapter concludes with a discussion on previous transitions used to feed SIW.

2.2 Design of an array antenna with longitudinal slots on the broad wall of a rectangular waveguide

Elliot [7] devised a procedure that allows for the design of a slotted waveguide antenna with longitudinal slots cut out of the broadside of the waveguide. Design equations were developed by replacing an array of slots cut out of a waveguide with an array of equivalent dipoles via Babinet's principle. These equations gave a relationship between the mode voltages and the slot voltages. Equations relating the self and mutual admittances of slots are also derived. Using these equations an iterative design procedure is developed.

Elliot [8] improved his slotted waveguide design procedure by determining how the voltage within the slot is induced. With the reciprocity theorem Elliot [8] developed equations that linked the slot voltage to the TE modes passing through the waveguide and

the mutual coupling of the slots. This new procedure no longer needed the equivalent dipoles and also allowed for the inclusion of dielectric-filled waveguides to be designed. Elliot and Loughlin [9] further improved the slotted waveguide design procedure by taking into account the higher order modes that scattered off adjacent slots. In waveguides of reduced height the resonant slot length increases, therefore the tip-to-tip distance between adjacent slots decreases. The higher order modes scattered off the slot do not necessarily attenuate to a negligible quantity and therefore their affect on the slot voltage must be taken into account. An additional term was added to the slot voltage equation improving the accuracy of the design procedure.

2.3 Substrate Integrated Waveguide

Cassivi *et al.* [11] analyzed substrate integrated waveguides (SIWs) using the BI-RME method combined with Floquet's theorem to determine the dispersion characteristics of the SIW. The SIW is composed of a substrate covered on the top and bottom with a thin metallic sheet and metallic via holes are used to simulate the side walls of a rectangular waveguide.

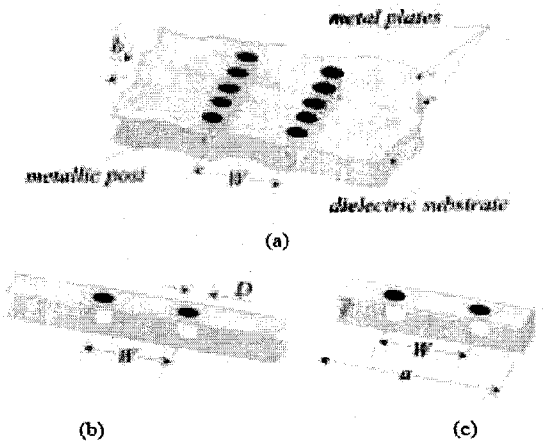

Figure 2.1: a) Sketch of a SIW. b) Periodic cell of SIW. c) Enclosed periodic cell.[11]

The SIW is a periodic structure; figure 2.1 shows a sketch of a SIW and of a periodic cell of a SIW. A generalized admittance matrix of the periodic cell is determined using the BI-RME method. Due to the periodic nature of the SIW, Floquet's theorem can be used to obtain an eigenvalue system. The eigenvalues give the propagation constants of the TE_{n0} modes propagating through the SIW and the eigenvectors give the pattern of the modal fields. Their work has shown that substrate integrated waveguides have the same basic guided wave characteristics as rectangular waveguides. They have derived empirical formulas which estimate the cutoff frequencies of the first two dominant modes of the SIW.

$$f_{c_{TE10}} = \frac{c_0}{2\sqrt{\varepsilon_r}}\left(a - \frac{d^2}{0.95 \cdot s}\right) \tag{2.1}$$

and

$$f_{c_{TE20}} = \frac{c_0}{\sqrt{\varepsilon_r}}\left(a - \frac{d^2}{1.1 \cdot s} - \frac{d^3}{6.6 \cdot s}\right) \tag{2.2}$$

Where a is the SIW width, d is the diameter of the via holes, s is the spacing between adjacent via holes and c_0 is the speed of light. Comparing equation (2.1) with the equation that determines the cutoff frequency of the dominant mode of rectangular waveguides, Cassivi *et al.* [11] have derived an equation that relates the width of a SIW to an equivalent width of a rectangular waveguide.

$$a_{RWG} = a - \frac{d^2}{0.95 \cdot s} \tag{2.3}$$

Substrate integrated waveguides are periodic structures which are much more complicated to design when compared to a conventional waveguide. Deslandes and Wu [1] have developed a simple design procedure which transforms an SIW into an

equivalent rectangular waveguide [1] using a commercially available finite element software package. This allows the designer to design a system using a conventional waveguide then follow their procedure to find an equivalent SIW to replace the rectangular waveguide.

Deslandes and Wu [1] have developed a method for determining the complex propagation constant of a SIW using the concept of surface impedance to model the rows of conducting cylinders which act as the sidewalls of a SIW [1]. The proposed model is solved using a method of moments and a transverse resonance procedure. An electromagnetic field of a TE_{10} mode wave propagating through a waveguide can be represented by a superposition of two waves propagating at an angle θ to the z-axis, in this case the direction in which the energy is propagating [1,12]. At the cutoff frequency the TEM waves are scattered by the two conducting rows of metallic via holes. Each row of via holes can be represented by a surface impedance z_s. Figure 2.2 shows a diagram of the two rows of via holes.

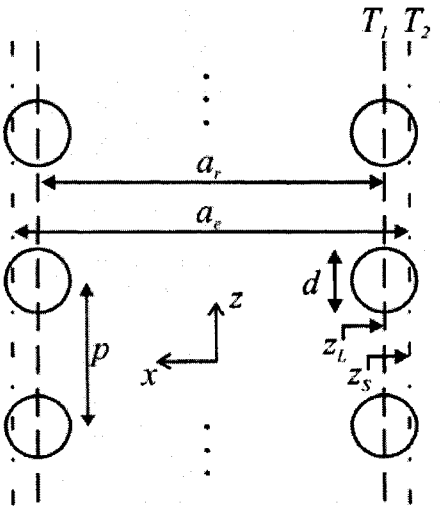

Figure 2.2: Diagram of via holes with the surface impedance concept [1].

A rectangular waveguide equivalent width a_e of the SIW can be calculated with a transverse resonance procedure. The propagation constant of the SIW can be characterized by the reflection coefficient of the row of via holes at the desired cutoff frequency. The reflection coefficient of the via holes at the cutoff frequency can be calculated with a method of moments technique. The novelty of this method is that the propagation constant of the SIW can be calculated both accurately and quickly. This method can be further used to extract not only the guided-wave properties of the SIW but also the leakage characteristics of the periodic structure. From these results design rules have been suggested to follow in order to minimize leakage and avoid bandgaps in the operating bandwidth and to overall assist the designer design substrate integrated waveguides. The first design rule is straight forward and states that the separation distance *s* must be larger than the via hole diameter *d*. The second design rule states that the separation distance must be smaller than a quarter wavelength at the cutoff frequency. In order to ensure negligible leakage loss between the metallic cylinders a third design rules states that the separation distance should be smaller than *2d*. Good experimental results were shown to validate the theory described above.

2.4 Substrate Integrated Waveguide Antennas with Longitudinal Slots

Yan *et al.* [13] have designed a 4x4 SIW slot antenna array. The whole antenna and feeding system are integrated in one substrate which leads to small size, low profile and low cost. Longitudinal slots were etched on the top metallic surface of a SIW making use of work done by Elliot [7,8,9]. They determined the equivalent width of a rectangular waveguide for a SIW through the following equations.

$$\bar{a} = \xi_1 + \frac{\xi_2}{\frac{s}{d} + \frac{\xi_1 + \xi_2 - \xi_3}{\xi_3 - \xi_1}} \tag{2.4}$$

where

$$\xi_1 = 1.0198 + \frac{0.3465}{\frac{a}{s} - 1.0684} \tag{2.5}$$

$$\xi_2 = -0.1183 - \frac{1.2729}{\frac{a}{s} + 1.2010} \tag{2.6}$$

$$\xi_3 = 1.0082 - \frac{0.9163}{\frac{a}{s} + 0.2152} \tag{2.7}$$

The equivalent width of a rectangular waveguide in terms of the width of the corresponding SIW is given by

$$a_{RWG} = \bar{a}a \tag{2.8}$$

where a is the width of the SIW. This method for determining the equivalent width is accurate to within 1%. This method is more accurate than the one described by Cassivi *et al.* [11] in equation (2.3). A picture of the antenna is given in figure 2.3. The antenna is fed through a network of microstrip lines feeding each SIW.

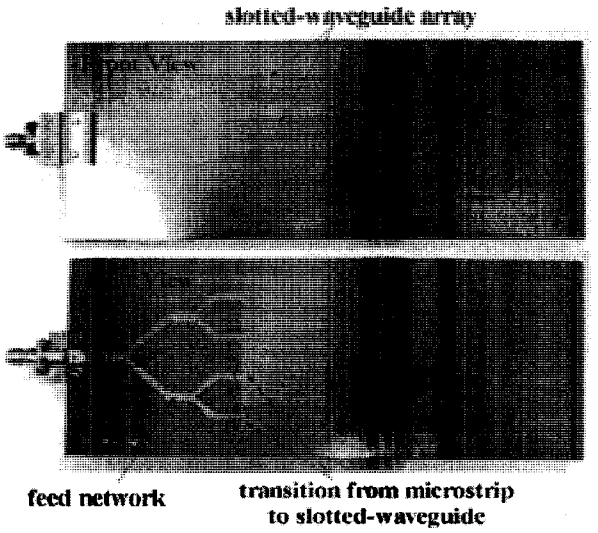

Figure 2.3: Front and rear view of the slotted SIW array antenna [13].

Results show a 10dB bandwidth of 600MHz centered at 10GHz, however the return loss at the center frequency is found to be 11dB. A significant part of the losses is due to the feed network of the antenna.

Weng *et al.* [14] have designed a 5-slot SIW antenna array for the Ku-band. Longitudinal slots are etched on the top metallic surface of an SIW in a manner similar to Yan [13]. The whole antenna is integrated on one substrate for small size and easy manufacturability. A picture of the antenna they built is given in figure 2.4.

Figure 2.4: Slotted SIW array antenna fed by a microstrip line [14].

Results show a 10dB bandwidth of 500MHz centered about 14.7GHz with a center frequency return loss of 20dB.

2.5 Transition between Microstrip Line and Substrate Integrated Waveguide

Deslandes and Wu [4] have presented a transition between a microstrip line and planar dielectric-filled waveguide fabricated on the same substrate. The microstrip line and planar form waveguide are connected together through a simple tapered transition. A diagram of this transition is given in figure 2.5.

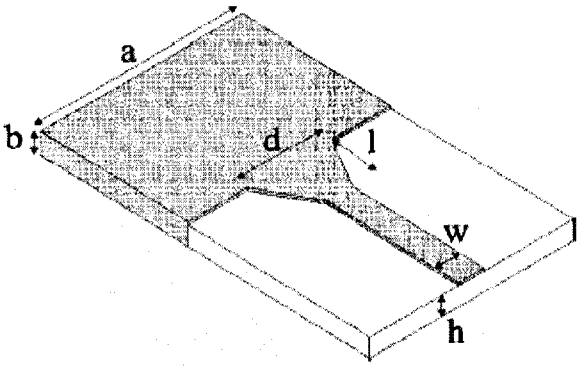

Figure 2.5: Transition between microstrip line and dielectric-filled waveguide [4].

The electric field profile of a microstrip line and rectangular waveguide are similar. A sketch of the field profiles of a microstrip line and waveguide are given in figure 2.6. Because the electric field profiles of the two different structures are similar, a tapered transition is well suited to match the two transmission lines.

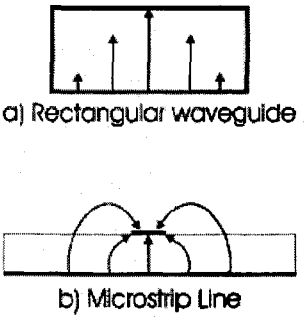

Figure 2.6: Electric field profiles of a rectangular waveguide and microstrip line [4].

Their results show a 12% bandwidth for a return loss less than 20dB centered around 28GHz with an insertion loss better than 0.3dB.

Nam *et al.* [15] have designed a transition between a microstrip line and a SIW using a tapered transition in the Ku-Band. The transition they designed is different than the one described above [4]. A sketch of transition is given in figure 2.7.

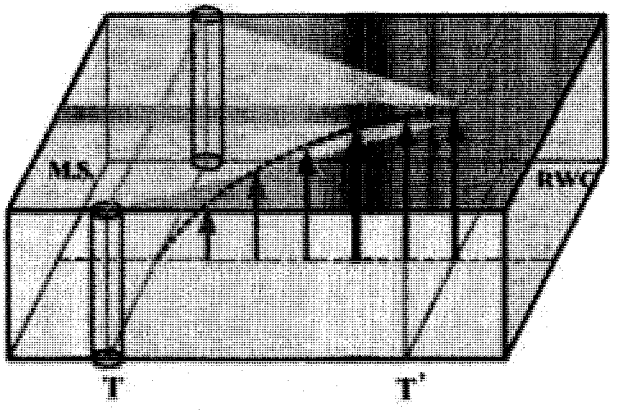

Figure 2.7: Transition between a microstrip line and a SIW [15].

In figure 2.7 the green colour on the top plane represents the metallic conductor and indicates how this tapered transition is etched. The red lines show how the electric field

varies along the transition. A picture of this transition that Nam *et al.* [15] have fabricated is shown in figure 2.8.

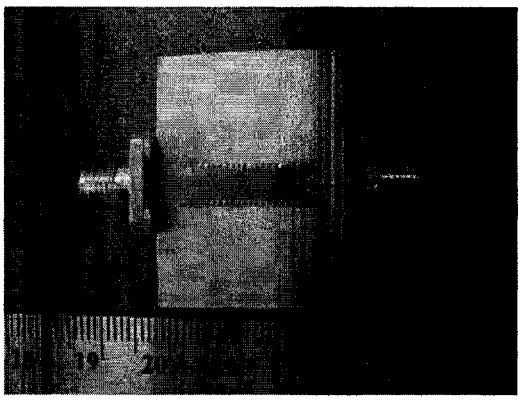

Figure 2.8: Back-to-back transition between a microstrip line to SIW [15].

Their results show a return loss of less than 15dB between the frequencies 11-14GHz for a back-to-back transition. Over the same frequency band the insertion loss better than 0.7dB for the back-to-back transition.

Ding and Wu [16] present a novel transition between a microstrip line and a SIW in a multi-layered substrate environment. Their design consists of a double-layered transition between a tapered ridged SIW and a tapered microstrip line. Also a two-stage, triple-layered transition is proposed to shorten the overall length of the microstrip to SIW transition. The transitions are designed by taken into account both impedance matching and field matching simultaneously. The characteristic impedance and guided wavelength of the transmission lines are computed using closed-form expressions based on a transverse resonance method. These results are used to develop a design procedure for the transition. A diagram of the transition is given in figure 2.9.

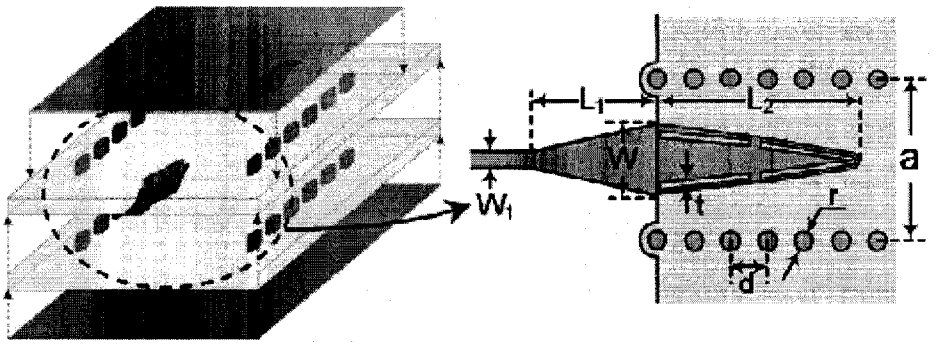

Figure 2.9: Transition between a microstrip line and a SIW. The transition consists of a tapered microstrip line and a tapered ridge waveguide [16].

The first part of the transition consists of a tapered microstrip line that leads into a tapered ridge SIW which is the second part of the transition. The tapered ridge narrows off and leads into the SIW. The tapered ridge consists of the three metallic grooves; refer to figure 2.9 for a visual reference. For the double-layered back-to-back transition a 14.5% bandwidth with a 15dB return loss is achieved centered about 25GHz with an insertion loss of 1.5dB.

Deslandes & Wu [5] have proposed a transition that connects a grounded coplanar waveguide to a SIW. The transition is composed of a current probe that descends from the grounded coplanar waveguide to the bottom ground plane of the SIW. The current flowing through the probe creates a magnetic field inside the SIW. This magnetic field matches the TE_{10} mode magnetic field in a waveguide and propagates through the SIW. A diagram of the transition between the two structures is given in figure 2.10.

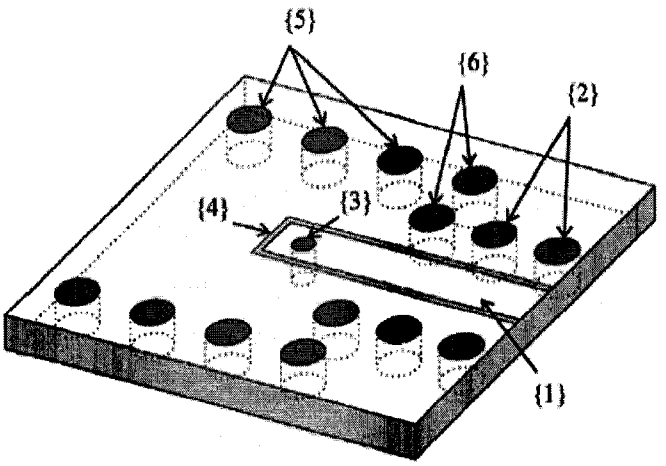

Figure 2.10: Transition between a grounded coplanar waveguide and a SIW with the use of a current probe [5].

Metallic via holes seen in figure 2.10 {5} form the sidewalls of the SIW. The current probe is indicated by {3} and the grounded coplanar waveguide is indicated by {1}. Metallic via holes {2} are placed on either side of the GCPW to simulate metallic sidewalls along the GCPW. These sidewalls suppress the unwanted leaky wave parallel-plate modes that may appear in the GCPW. The SIW is terminated with a short circuit formed by metallic via holes indicated by {6}. The current probe must be located a quarter-wavelength from the short, this way the current probe sees an infinite impedance looking back towards the short circuit. Experiments performed at 28GHz on this transition show a 10% bandwidth with an insertion loss that is less than 0.73dB over the frequency range of interest.

Chapter 3

Analysis & Design of Slotted Substrate Integrated Waveguide Antennas

3.1 Design Overview

The goal of this thesis is to present the design of a slotted substrate integrated waveguide array antenna. The antenna is fed with a stripline, therefore a transition between a stripline and a SIW must be designed. For this thesis a vertical transition consisting of a single metal-plated via hole is connected at the edge of the stripline down to the ground plane. Given the circuit requirements and available fabrication facility it is not be possible to attach an SMA connector to the stripline, the SMA connector must be soldered onto a microstrip line. To overcome this problem we must design a transition between a microstrip line and a stripline. A simple tapered transition between the two transmission lines is used.

The design procedure is as follows: first we choose a design frequency which determines an appropriate waveguide width and we must also choose a substrate. Using Elliot's [8,9] design procedure for a dielectric-filled slotted waveguide antenna we find the appropriate dimensions and locations of the 8 slots that are cut out of the broadside of the rectangular waveguide. Elliot's [8,9] procedure takes into account the self admittance, slot voltage, mode voltage and mutual coupling between adjacent slots in order to achieve good matching as well as a good radiation pattern. Once the slotted waveguide antenna has been properly designed, a stripline enclosed with vertical metallic walls, sometimes referred to as a rectangular coaxial cable, is used to feed the antenna. A vertical transition between the 50Ω shielded stripline and the slotted waveguide antenna is the second main design challenge of the circuit. The design of the vertical transition is based upon a

similar transition [17] between a coaxial cable and a waveguide. A microstrip and the transition between a microstrip and stripline is designed to allow the SMA connector to be soldered to the circuit. Once the microstrip line, stripline and waveguide antenna have been successfully designed the next step in the design procedure is to replace the vertical metallic walls that surround the stripline and waveguide with a row of copper-plated via holes.

3.2 A Waveguide-Fed Slot

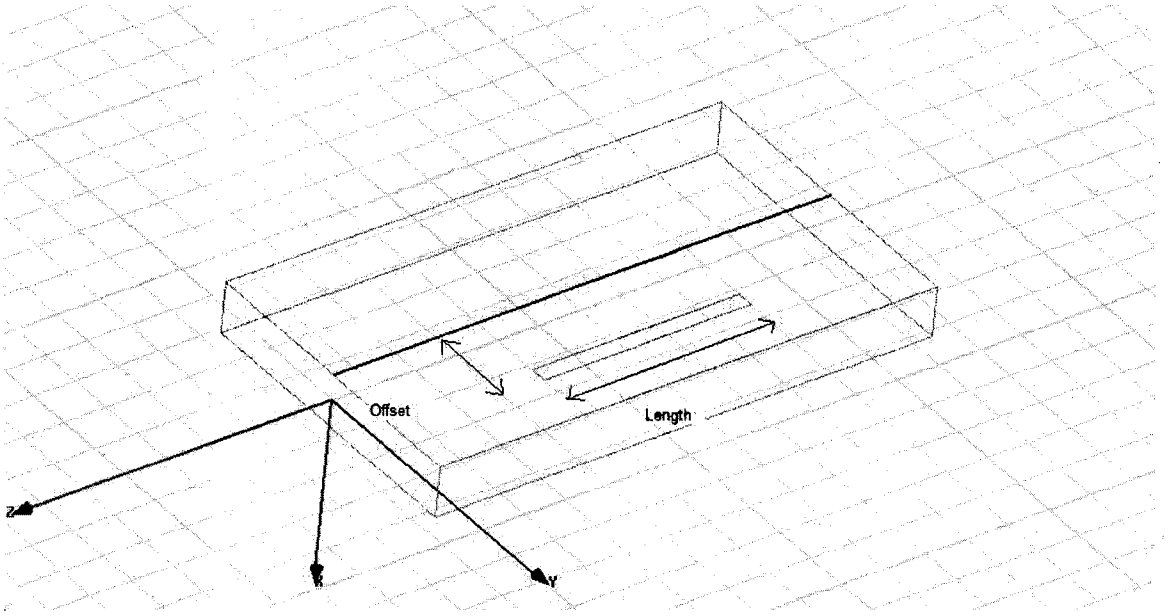

Figure 3.1: Longitudinal slot cut out of a piece of waveguide.

A slot cut out of a waveguide is one of the most fundamental types of aperture antennas. Figure 3.1 shows a slot cut out of the broadside of a waveguide. If the waveguide is excited with TE_{10} mode wave traveling in the z-direction, the normalized field components are [12]

$$H_z = j\cos\left(\frac{\pi x}{a}\right)\cdot e^{j(\omega t-\beta z)}$$
$$H_x = -\frac{\beta}{\pi/a}\sin\left(\frac{\pi x}{a}\right)\cdot e^{j(\omega t-\beta z)} \quad (3.1)$$
$$E_y = \frac{\omega\mu_0}{\pi/a}\sin\left(\frac{\pi x}{a}\right)\cdot e^{j(\omega t-\beta z)}$$

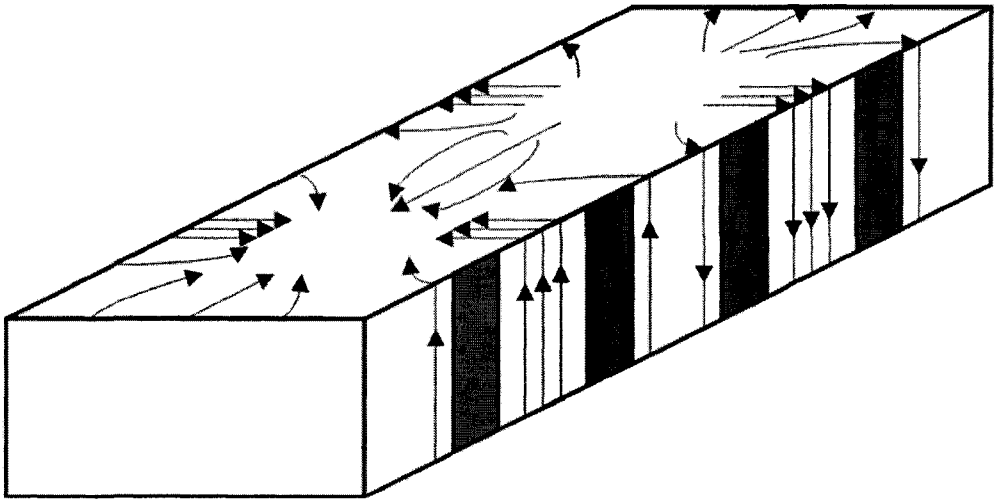

Figure 3.2: Instantaneous current flow of TE_{10} mode waveguide [3].

Figure 3.2 shows the instantaneous current flow on the waveguide surface when excited by a TE_{10} mode wave. The current distribution pattern propagates through the waveguide with time. If a narrow slot is cut longitudinally into the broadside of the waveguide, as shown in figure 3.1, then the slot interrupts the x-directed current that flows on the surface of the broadside of the waveguide [18-21]. This interruption in current causes an electric field to develop within the slot. A slot cut out along the centerline of the waveguide disrupts a very small amount of current and a very weak electric field develops across the slot resulting in a negligible amount of radiation. However, as we displace the slot from the centerline a larger amount of current is interrupted and thus a

stronger electric field develops across the slot resulting in a larger amount of energy coupled into space [7,8]. Therefore the greater the slot is displaced from the centerline, the greater the amount of radiation emanates from the slot. This is a very interesting and useful result. It allows the designer the ability to control the amount of radiation from a slot by varying the slot displacement from the waveguide centerline.

Previous works [18-24] have shown that the electric field induced in a longitudinal slot cut out of the broadside of a waveguide, when the waveguide is excited with a TE_{10} mode wave, is symmetrical around the center of the slot. If the slot length is not too far off resonance, the electric field within the slot can be approximated with the following equation [8]:

$$E_x = \frac{V^s}{w}\cos\left(\frac{\pi z'}{l}\right) \tag{3.2}$$

Where V^s is the voltage across the center the center of the slot, w is the width of the slot, l is the length of the slot and z' represents the position along the z-axis where the origin is taken to be the line that bisects the slot, keeping in mind that the slot is directed along the z-axis. The symmetry of the electric field in the slot implies that a longitudinal slot in the broadside of a waveguide can be thought of as a shunt element in a two-wire transmission line [7,8]. The scattering of a TE_{10} mode wave caused by the slot is equivalent to the scattering caused by a shunt element in a two-wire transmission line.

Using this information one is able to find a relation between the backscattered mode amplitude B_{10} and the forward-scattered mode amplitude C_{10} to the electric field induced in the slot when a TE_{10} mode wave is incident upon the slot.

$$B_{10} = C_{10} = \frac{\int_{slot} (E_1 \times H_2) \cdot dS}{2\int_{S_1} (E_{10} \times H_{10}) \cdot 1_z dS_1} \tag{3.3}$$

Where E_1 can be found in equation (3.2) and

$$H_2 = 1_z j \cos\left(\frac{\pi x'}{a}\right) \cdot e^{-j\beta_{10} z}$$

$$E_{10} = 1_y \frac{\omega\mu_0}{\pi/a} \sin\left(\frac{\pi x'}{a}\right) \tag{3.4}$$

$$H_{10} = 1_x \frac{\beta_{10}}{\pi/a} \sin\left(\frac{\pi x'}{a}\right)$$

After integrating and simplifying equation (3.3) results in

$$B_{10} = -K \frac{(\pi/2kl) \cdot \cos(\beta_{10} l)}{(\pi/2kl)^2 - (\beta_{10}/k)^2} \sin\left(\frac{\pi x}{a}\right) V_s \tag{3.5}$$

where

$$K = \frac{2(\pi/a)^2}{j\omega\mu_0(\beta_{10}/k)(ka)(kb)}, \quad k = \omega\sqrt{\mu_0 \varepsilon} \tag{3.6}$$

Equation (3.5) gives a relationship between electric field and the backscattered amplitude mode, note that the x variable in eq.(3.5) is the offset displacement from the center of the waveguide [8].

3.3 The Design Equations of a Linear Slotted Waveguide Array

There are two main types of slotted waveguide arrays with longitudinal slots: a standing-wave fed array of slots and a traveling-wave fed array of slots. A standing-wave fed array of linear slots is composed of an array of slots spaced apart by a distance of $\lambda_g/2$, where λ_g is the guide wavelength of the TE_{10} mode propagating through the waveguide. If the

spacing between the slots is anything other than $\lambda_g/2$ then the array is said to be traveling-wave fed [7,25]. This thesis presents the design of a standing-wave fed linear array of slots cut in the broadside of the SIW.

When designing an array of waveguide-fed slots the designer must be able to control the power radiated by each slot, ensure that all slots are resonating at the design frequency and that the sum of all slot admittances equal the characteristic admittance of the waveguide. The power radiated by each slot is directly related to the amplitude of the electric field induced in the slot [7,8,21-25]. The electric field amplitude in the slot can be controlled by the slot displacement x from the centerline of the waveguide. To ensure that the slots are resonating at the design frequency the slot lengths must be appropriately adjusted, usually to about $\lambda_g/2$. It is desirable to have the active admittances of all slots to be purely real. The active admittance of a slot is a function of the slot's offset and length. It is also dependent upon the mutual coupling from the other slots cut out of the waveguide [8,26,27]. The designer must carefully choose the appropriate slot lengths and offsets so that all the active admittances of the slots are purely real and resonating and that their sum is equal to the characteristic admittance of the waveguide to ensure good impedance matching. At the same time the designer can also control the amount of power radiated by each slot while maintaining the above two conditions. This allows for control over the sidelobe levels and half-power beam width of the radiation pattern.

The symmetry of equation (3.2) allows one to view the waveguide-fed slot as a shunt admittance on a two wire transmission line [8,9]. The symmetrical scattering off the shunt admittance modeling the n^{th} slot in an array of N slots can be modeled in terms of its active admittance Y_n.

$$B = C = -\frac{1}{2}\frac{Y_n}{G_0}V_n \tag{3.7}$$

Where G_0 is the characteristic admittance of the waveguide and V_n is the mode voltage at the center of the slot. Equations (3.5) & (3.7) can be combined by requiring B_{10} and B to have the same phase at all points along the z-axis and that the backscattered power levels are the same [7,8]. The result is a principle design equation that will be used in the design the antenna.

$$\frac{Y_n}{G_0} = K_1 f_n \frac{V_n^s}{V_n} \tag{3.8}$$

where

$$K_1 = \frac{1}{j(a/\lambda)}\sqrt{\frac{2(k/k_0)}{\eta G_0(\beta_{10}/k)(ka)(kb)}} \tag{3.9}$$

in which η is the free space impedance, and

$$f_n = \frac{(\pi/2kl_n)\cdot\cos(\beta_{10}l_n)}{(\pi/2kl_n)^2 - (\beta_{10}/k)^2}\cdot\sin(\frac{\pi x_n}{a}) \tag{3.10}$$

We have derived equations (3.8, 3.9, and 3.10) which gives a relationship between the electric field induced in the slot and the active admittance of the slot. It is now desirable to determine the causes of the electric field induced in the n^{th} slot in a linear array of N slots. The total slot voltage can be decomposed into four parts

$$V_n^s = V_{n,1}^s + V_{n,2}^s + V_{n,3}^s + V_{n,4}^s \tag{3.11}$$

The first part of the slot voltage is due to the TE_{10} mode wave of complex amplitude A_{10} incident upon the slot coming from z=-∞ in the positive z-direction. Since we are designing a standing-wave fed array of linear slots in the waveguide there is a reflected TE_{10} mode wave of complex amplitude D_{10} incident upon the slot coming from z=+∞ in

the negative z-direction. This reflected wave will contribute to the second part of the slot voltage. The third contribution to the total slot voltage comes from the mutual coupling of the other N-1 slots in the waveguide. The fourth and final contribution to the total slot voltage comes from the internal higher order modes scattering off adjacent slots [9,28]. Consider the first case with a TE_{10} mode wave of complex amplitude A_{10} incident upon the n^{th} slot with all other N-1 slots covered with electrical tape and after the n^{th} slot the waveguide is terminated in a matched load. The equivalent transmission line circuit of this situation consists of the self-admittance of the slot in parallel with the characteristic admittance of the waveguide and can be represented with the following equation:

$$\frac{Y}{G_0} = -\frac{2(B/A)}{1+(B/A)} \tag{3.12}$$

where A is the incident wave upon the slot and B is the backscattered wave caused by the discontinuity at the slot. This equation is still valid if A & B are replaced with A_{10} & B_{10}. Performing this substitution and rearranging this equation leads to

$$B_{10}^n = \frac{\frac{Y}{G_0}(x_n, l_n)}{2+\frac{Y}{G_0}(x_n, l_n)} A_{10}^n \tag{3.13}$$

where x_n and l_n is the offset and length of the n^{th} slot respectively. In the previous section we have determined that the scattering off the slot in question is symmetrical, $B_{10} = C_{10}$. Thus equation (3.13) allows one to calculate the scattering matrix of the slot, which is characterized by a two-port microwave circuit as a shunt admittance, if the normalized self-admittance of the slot as a function of the offset x_n and length l_n is known [7-9]. The same equation applies to the reflected wave D_{10}. Combining equations (3.5, 3.10, 3.13) we obtain

$$V_{n,1}^{s} = \frac{1}{Kf_n} \cdot \frac{\frac{Y}{G_0}(x_n, l_n)}{2 + \frac{Y}{G_0}(x_n, l_n)} A_{10}^{n} \tag{3.14}$$

The second part of the slot voltage due to the reflected wave D_{10} can be found by simply replacing A_{10} with D_{10}.

$$V_{n,2}^{s} = \frac{1}{Kf_n} \cdot \frac{\frac{Y}{G_0}(x_n, l_n)}{2 + \frac{Y}{G_0}(x_n, l_n)} D_{10}^{n} \tag{3.15}$$

The third part of the slot voltage is due to the mutual coupling of the other N-1 slots. This voltage was derived analytically in [7] with the aid of the reciprocity theorem and is given by

$$V_{n,3}^{s} = -j(\beta_{10}/k)(k_0 b)(a/\lambda)^3 \cdot \frac{1}{f_n^2} \cdot \frac{\frac{Y}{G_0}(x_n, l_n)}{2 + \frac{Y}{G_0}(x_n, l_n)} \cdot \sum_{m=1}^{N}{}' V_m^{s} g_{mn}(x_m, l_m, x_n, l_n) \tag{3.16}$$

where g_{mn} is given by

$$g_{mn} = \int_{-k_0 l_m}^{k_0 l_m} \cos\left(\frac{z_m'}{4l_m/\lambda_0}\right)\left\{\frac{1}{4l_n/\lambda_0}\left[\frac{e^{-jk_0 R_1}}{k_0 R_1} + \frac{e^{-jk_0 R_2}}{k_0 R_2}\right] + \left[1 - \frac{1}{(4l_n/\lambda_0)^2}\right] \cdot \int_{-k_0 l_n}^{k_0 l_n} \cos\left(\frac{z_n'}{4l_n/\lambda_0}\right) \frac{e^{-jk_0 R}}{k_0 R} dz_n'\right\} dz_m' \tag{3.17}$$

Notice the prime on the summation sign in equation (3.16), this indicates that the term m=n is excluded from the summation. We have also introduced the substitute variable $z=k_0\zeta$ in equation (3.17). The variable R is the distance between the point $P_m(0,0,\zeta'_m)$ and $P_n(0,0,\zeta'_n)$. The variable R_1 is the distance between the point $P_m(0,0,\zeta'_m)$ and $P_{n,1}(0,0,l_n)$.

The variable R_2 is the distance between the point $P_m(0,0,\zeta'_m)$ and $P_{n,2}(0,0,-l_n)$. Figure 3.3 graphically shows the distances R, R_1 and R_2.

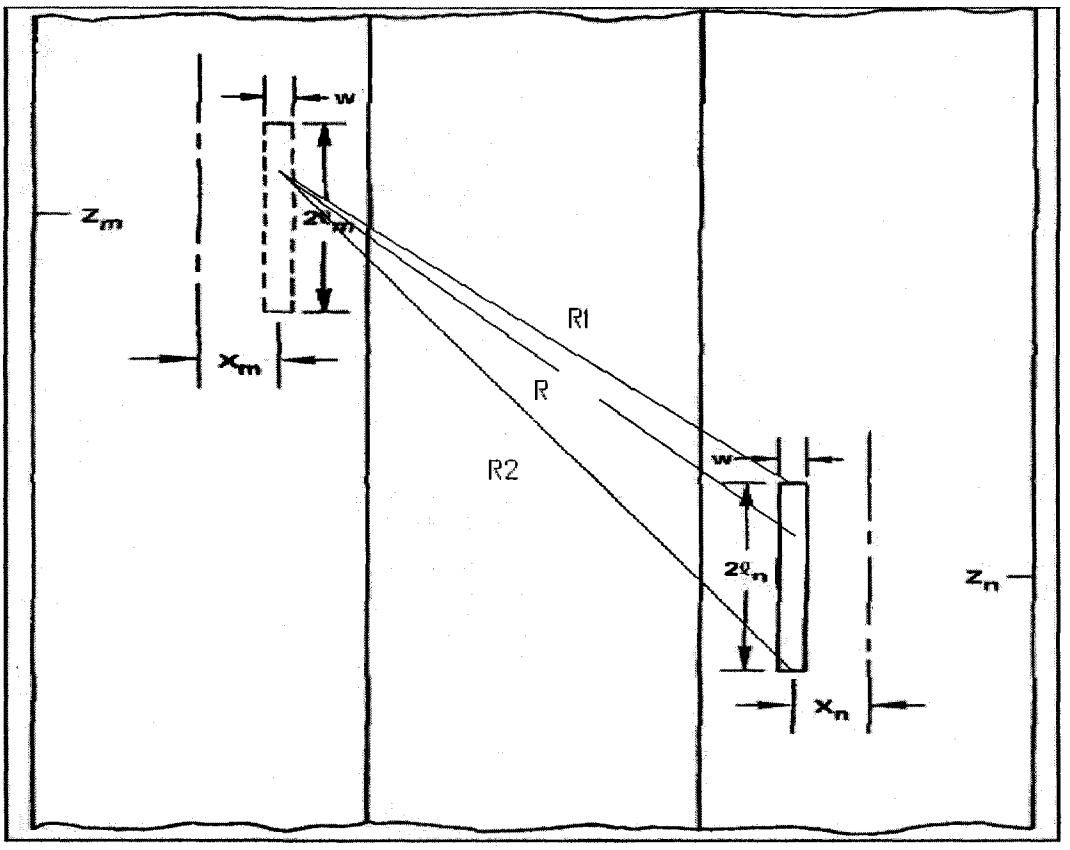

Figure 3.3: Graphically description of slot distances R, R_1, and R2 [8].

When dealing with a TE_{10} mode wave it is only the *a* dimension of the waveguide that determines the cutoff frequency [12]. Although the *b* dimension does not have an effect on the cutoff frequency of the TE_{10} mode wave it does affect the resonant length of a slot cut out of the broadside of the waveguide [9]. Elliot and Loughlin [9] have shown that as the *b* dimension decreases the resonant slot length increases. For this thesis the design procedure was to design a slotted waveguide array antenna and using those results transform the waveguide into an equivalent substrate integrated waveguide. One main

difference between a regular rectangular waveguide and a SIW is that the *b* dimension is considerably smaller for the SIW. Therefore when designing the slotted rectangular waveguide antenna, the *b* dimension must be chosen to match the substrate thickness of the slotted SIW antenna. This substantial decrease in the *b* dimension results in an increase in the resonant length of the slot cut out of the waveguide [7,9]. The frequency of course remains unchanged and the distance between the slots is still $\lambda_g/2$, thus the tip-to-tip distance between adjacent slots will decrease. Earlier slotted waveguide theory [7] states that the higher order modes scattered off a slot will attenuate to a negligible quantity before reaching adjacent slots in a standing-wave fed antenna. Due to the fact that the tip-to-tip distance between adjacent slots decreases with a decrease in the dimension *b* one can no longer assume that the higher order modes scattered of a slot will have a negligible contribution to the slot voltage of adjacent slots. Previous work on this subject [9,28] has shown that the higher order modes coupling to adjacent slots consist of just the TE_{20} mode. This higher order mode coupling is accounted for by including its affect on the slot voltage and is the fourth part of the slot voltage found in equation (3.11). It must be noted that this internal mutual coupling only affects the two slots adjacent to the slot in question unlike the external mutual coupling, the third part of equation (3.11), where all other slots are affected. The fourth part of this slot voltage was analytically determined in [9] with the application of the reciprocity theorem and was found to be

$$V_{n,4}^{s} = -j\frac{(\beta_{10}/k)}{(\gamma_{20}/k)}e^{-(\gamma_{20}/k)kd}\left[\frac{1}{f_n^2}\cdot\frac{\frac{Y}{G_0}(x_n,l_n)}{2+\frac{Y}{G_0}(x_n,l_n)}\right]\cdot\left[h_n h_{n-1}V_{n-1}^{s}+h_n h_{n+1}V_{n+1}^{s}\right] \tag{3.18}$$

where

$$\gamma_{20} = \sqrt{(2\pi/a)^2 - k^2} \tag{3.19}$$

and

$$h(x,l) = 2\frac{(\lambda/4l)\cosh(\frac{\gamma_{20}}{k}kl)}{(\gamma_{20}/k)^2 + (\lambda/4l)^2}\cos(\frac{2\pi x}{a}) \tag{3.20}$$

For a standing-wave fed slotted waveguide array antenna we have the two following equations that represent the sum of the active admittances of slots from the n^{th} slot to the N^{th} slot and the $(n+1)^{th}$ slot to the N^{th} slot, where the total number of slots is N.

$$\sum_{i=n}^{N}\frac{Y_i}{G_0} = \frac{A_{10}^n - (B_{10}^n + D_{10}^n)}{A_{10}^n + (B_{10}^n + D_{10}^n)} \tag{3.21}$$

and

$$\sum_{i=n+1}^{N}\frac{Y_i}{G_0} = \frac{(A_{10}^n + C_{10}^n) - D_{10}^n}{(A_{10}^n + C_{10}^n) + D_{10}^n} \tag{3.22}$$

It is a simple matter of subtracting the two equations (3.21 & 3.22) to develop an expression for the active admittance of the n^{th} slot.

$$\frac{Y_n}{G_0} = -\frac{2B_{10}^n}{A_{10}^n + B_{10}^n + D_{10}^n} \tag{3.23}$$

We have already stated that the scattering of the slot is symmetrical and $B_{10}=C_{10}$. Using this knowledge in combination with equations (3.5, 3.14, 3.15) we can rearrange equation (3.23) to give

$$\frac{Y_n}{G_0} = \frac{2f_n^2(x_n,l_n)}{\frac{2f_n^2(x_n,l_n)}{\frac{Y_n}{G_0}(x_n,l_n)} + MC_n} \tag{3.24}$$

where MC_n is the mutual coupling term that represents both the external coupling from all other slots in the waveguide and the internal higher order mode coupling from the two

adjacent slots.

$$MC_n = j(\beta_{10}/k)(k_0 b)(a/\lambda)^3 \cdot \sum_{m=1}^{N}{}' \frac{V_m^s}{V_n^s} g_{mn}(x_m, l_m, x_n, l_n) + j\frac{(\beta_{10}/k)}{(\lambda_{20}/k)} e^{-(\gamma_{20}/k)kd}[h_n h_{n-1}\frac{V_{n-1}^s}{V_n^s} + h_n h_{n+1}\frac{V_{n+1}^s}{V_n^s}] \quad (3.25)$$

Equation (3.24) is the second principle expression for slotted waveguide antennas. Equation (3.24) in conjunction with equation (3.8) is used to design a slotted waveguide antenna.

3.4 Design Procedure of a Broadside Linear Array of Longitudinal Slots

In the previous section we have discussed the design equations for a broadside slotted waveguide array. We will now make use of a design procedure developed by Elliot [7-9] to design a standing-wave fed slotted waveguide array of longitudinal slots. Let there be N slots spaced $\lambda_g/2$ apart from one another. The designer can obtain a desired radiation pattern by appropriately controlling the slot voltage of the individual slots. There are different methods for controlling the radiation pattern of an array antenna. The simplest method is a uniform array antenna where the elements in the array radiate the same amount of power [25]. This results in the antenna having the maximum directivity, however the sidelobe levels are stuck at 13.5dB below the main beam and cannot be reduced any further. One can also divide the available power to the slots according to a Chebychev distribution [25,29,30]. This allows the designer to control the sidelobe levels. In certain applications it is necessary that the sidelobes be reduced to a certain percentage of power with respect to the main beam. As the sidelobes become weaker the main beam of the antenna loses its directivity, this is the price that must be paid for

reduced sidelobes. Another method is the binomial distribution which in theory eliminates the sidelobes completely, however, as before, the directivity of the antenna is considerably decreased [12].

Let us assume that the desired radiation pattern has been decided on and that the corresponding slot voltage distribution V^s_n is known. The mode voltage V_n has a common value for all slots except for an alternation in sign. This is due to the fact that the slots have been resonantly spaced apart by $\lambda_g/2$. This alternation is sign can be compensated for by simply switching the direction of the offset. Inspecting equations (3.8 & 3.10) shows that this is indeed true, the $sin(\pi x_n/a)$ term in equation (3.10) is what is responsible for this sign alternation, remembering that x_n is the offset parameter [7]. It is desired to have the main beam of the antenna radiate at the broadside of the antenna. This requires that all elements in the antenna array have the same phase. The requirement is fulfilled by ensuring that the spacing between elements is $\lambda_g/2$. Since the slot voltage V^s_n has the same phase for all the slots, the active admittances will also have the same phase for all slots. This can be seen by inspecting equations (3.8-3.10). It is desirable to have all elements radiating as efficiently as possible, thus it is necessary to design the antenna so that the active admittance of all slots is purely real.

Referring to equation (3.24) we notice that in order to calculate the active admittance of a slot the self-admittance of an isolated slot must be known. In fact we must characterize the self-admittance of an isolated slot for different values of offset x_n and length l_n. For this thesis we take advantage of commercially available software which allows for the simulation of high frequency circuits, in particular the Finite Element Method based software package Ansoft HFSS. To simulate the isolated slot a piece of waveguide of

length λ_g is used with the slot cut out in the middle at z=0, see figure 3.4. At $z=-\lambda_g/2$ the waveguide is fed with a TE_{10} mode wave, at $z=\lambda_g/2$ the waveguide is terminated with a absorbing boundary condition (ABC). This will absorb all fields that reach the $z=\lambda_g/2$ plane and act like a semi-infinite waveguide or alternatively as a matched waveguide. Therefore the only discontinuity in the waveguide is the slot and thus all the scattered fields are due to the slot alone. In the previous sections we have already stated that the slot voltage distribution is symmetrical and thus the scattering by the slot is symmetrical and can be modeled as a shunt element. This allows one to model the self-admittance of the slot with the following equation [8]

$$\frac{Y}{G_0} = \frac{-2\frac{B_{10}}{A_{10}}}{1+\frac{B_{10}}{A_{10}}} = \frac{-2S_{11}}{1+S_{11}} \tag{3.26}$$

The self-admittance data of an isolated slot was generated by varying the offset while keeping the length constant and measuring the S-parameters, then varying the length while keeping the offset constant and measuring the S-parameters. Once the self-admittance data of an isolated slot as a function of offset and length has been characterized we can begin the iterative procedure of slotted waveguide array design set out by Elliot [7,8]. The goal of the procedure is to determine the lengths and offsets of all N slots such that the desired radiation pattern is achieved through the appropriate slot voltage distribution, the slots are resonating at the design frequency and thus the active admittances are purely real and that the sum of the normalized active admittances of all N slots add to unity in order to achieve good matching between the slots and the waveguide. To begin with we choose initial offsets and lengths. It is acceptable to start off with slots

on the centerline (offset value of zero) and resonant lengths equal to $\lambda_g/2$. First the mutual coupling term, equation (3.25), is calculated with the chosen offsets and lengths for each slot using the desired slot voltage distribution V_n^s/V_m^s known from the pattern requirements. The next step is to perform a computer search using equation (3.10) and the self-admittance data and find the couplet (x_n, l_n) that makes the denominator of equation (3.24) purely real. There is a continuum of couplets (x_n, l_n) that satisfy this condition. This same procedure can be followed for the p^{th} slot that gives a continuum of couplets (x_p, l_p). From these sets of couplets, selecting the couplets that satisfy equation (3.8) rewritten here in ratio form must be done.

$$\frac{Y_p^a / G_0}{Y_n^a / G_0} = \frac{f_p V_p^s V_n}{f_n V_n^s V_p} \tag{3.27}$$

At the same time the matching condition must be satisfied, thus from the set of couplets that make the denominator of equation (3.24) purely real and that satisfy equation (3.27) selecting the set of couplets such that the sum of the active admittances equal unity must be performed.

$$\sum_{n=0}^{N} \frac{Y_n^a}{G_0} = 1 \tag{3.28}$$

This process is repeated except this time instead of choosing the slots along the centerline (zero offset) and resonant lengths ($2l=\lambda_g/2$), the new set of couplets that have been just found will be used to calculate the mutual coupling term in equation (3.25). This process is iterated until the offsets and lengths of each individual slot converge to a specific value. Once the set of couplets (x_n, l_n) converge to a final value the design process is complete and the necessary information, that being the size and location of the slots, is known, the slotted waveguide array antenna will have been designed [7].

3.5 Antenna Feed Structure

This section of the thesis deals with the feeding structure of the antenna. The slotted dielectric-filled waveguide antenna is embedded in a planar circuit so that it can be easily connected with other microwave circuits. The specific planar circuit consists of two substrates stacked on top of each other. There is a ground plane on the bottom and top of this double-layered substrate with slots cut out of the top ground plane. There are numerous ways in which one can feed such an antenna. One of the most common feeding methods is through the use of a tapered transition that connects a microstrip line to the dielectric-filled waveguide. Figure 3.4 shows a diagram of such a transition.

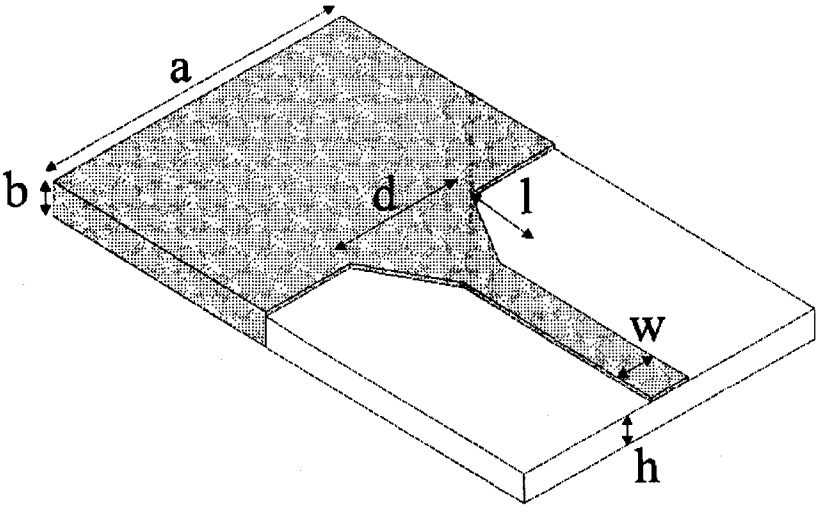

Figure 3.4: Transition between microstrip and dielectric-filled waveguide [4].

Deslandes *et al.* [4] have adopted such a transition in their work. The tapered section transforms the quasi-TEM mode of the microstrip line into a TE_{10} mode in the waveguide. The electric fields of the two different structures are oriented in the same direction and have similar profiles [4]. This allows for relatively good matching between

the two transmission lines. The dimensions of the proposed tapered transition in [4] are not well defined and will certainly change for different types of substrates, waveguide dimensions, frequency, etc. Therefore in order to design the transition it will be necessary to perform computer simulations to determine the appropriate length *l* and width *d* (see figure 3.4) which will give an optimum bandwidth and s-parameter characteristics.
For this thesis it was decided that the waveguide antenna will be fed with a rectangular coaxial cable integrated within the substrate. Chen [31] has done work determining the impedance properties of such transmission lines. Figure 3.5 shows a cross sectional diagram of a rectangular coaxial line.

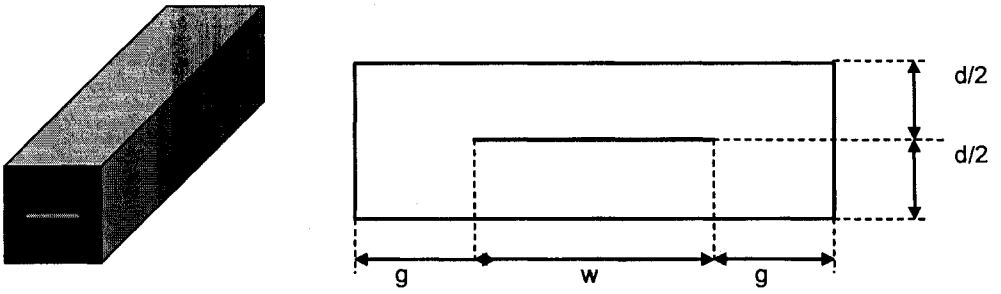

Figure 3.5: Rectangular Coax Line [32].

The structure of a rectangular coaxial line is very similar to that of a stripline, in fact the only difference between the two structures are the metallic sidewalls of the rectangular coax which enclose the inner conductor of the transmission line. The inner conductor is symmetrically placed inside the outer conductor. If the width of the both the inner conductor and outer conductor is substantially greater than its height then the fields of the rectangular coax are very similar to that of a shielded stripline [31]. In microwave circuits

there are usually many different types of transmission lines and microwave devices closely spaced together within the substrate. This gives rise to the important issue of crosstalk that can decrease the performance of the circuit. Enclosing the stripline with metallic walls has the additional advantage of shielding the propagating signal from other microwave devices within the same substrate and thus can significantly reduce the crosstalk phenomena.

Through the method of conformal transformation Chen [31] has derived equations which can be used to calculate the characteristic impedance of rectangular lines. The characteristic impedance of a rectangular line, when the inner conductor is symmetrically placed within the outer conductor, can be calculated through the following equation

$$Z = \frac{\sqrt{\mu/\varepsilon}}{2\left(\frac{f}{g}+\frac{w}{h}\right)+4\left(\frac{C_{f1}}{\varepsilon}+\frac{C_{f2}}{\varepsilon}\right)} \tag{3.29}$$

where

$$C_{f1} = \frac{\varepsilon}{\pi}\left[\log\frac{g^2+h^2}{4h^2}+2\left(\frac{h}{g}\right)\arctan\left(\frac{g}{h}\right)\right] \tag{3.30}$$

and

$$C_{f2} = \frac{\varepsilon}{\pi}\left[\log\frac{g^2+h^2}{4h^2}+2\left(\frac{g}{h}\right)\arctan\left(\frac{h}{g}\right)\right] \tag{3.31}$$

Where h is the height between the bottom of the outer conductor to the bottom of the inner conductor, because of the symmetry of the rectangular line the height h is the same from the top of the inner conductor to the top of the outer conductor, g is the length between the edge of the inner conductor to the sidewall of the outer conductor and f is the thickness of the inner conductor. Refer to figure 3.5 for a visual representation of the

above mentioned variables.

Using equations (3.29-3.31) a shielded stripline can be designed to have a characteristic impedance of 50Ω. A transition must be developed in order to efficiently transfer the signal propagating along the shielded stripline to the slotted waveguide antenna. For this thesis a vertical transition is proposed to connect the two dissimilar structures. The design of the proposed transition will borrow ideas from previous work [17,32-43] on transitions that connect a coaxial cable to a waveguide through the use of a probe.

Harrington [17] has studied different types of vertical transitions which connect a coaxial cable to a waveguide. The geometry of one particular transition can be seen in figure 3.6.

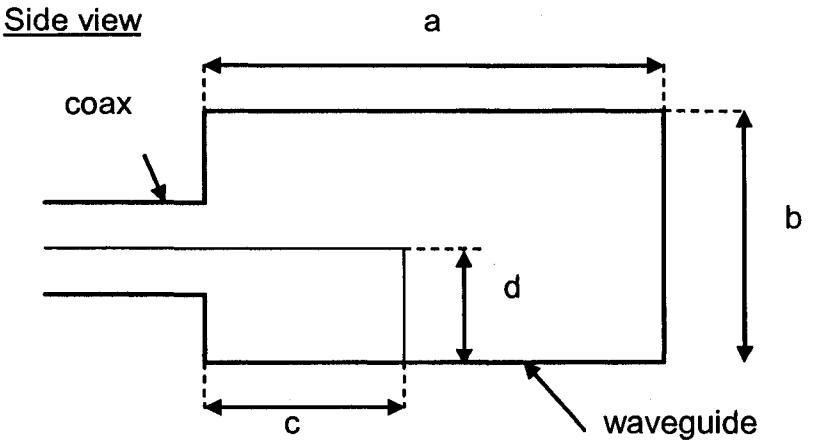

Figure 3.6: Transition between a coaxial cable and a waveguide [32].

The inner conductor of the coaxial cable is extended into the waveguide a distance *c* through and opening in the sidewall of the waveguide. The inner conductor is then bent 90° and continues down a distance *d* to the ground plane. Harrington [17] has derived an equation which computes the input resistance seen by the coaxial cable looking into the

waveguide.

$$Z_i = \frac{b}{a}(Z_0)_{01}\left[\frac{\sin\left(\pi c/a\right)\sin(kd)}{kb\cos\left(k(c+d)\right)}\right]^2 \tag{3.32}$$

where a and b are the waveguide dimensions, $(Z_0)_{01}$ is the waveguide impedance, k is the wave number, c is the distance the inner conductor of the coaxial cable extends into the waveguide, and d is the distance the inner conductor is above the ground plane of the waveguide.

This closed form equation allows the designer to quickly design a transition between a coaxial cable to a waveguide without having to perform tedious computer simulations. The proposed transition in this thesis takes advantage of this equation by using the same geometry seen in figure 3.6 by replacing the coaxial cable with a shielded stripline. The inner conductor of the shielded stripline extends into the waveguide a distance c. The inner conductor is terminated with a metallic cylinder, a metal-plated via hole that connects the inner conductor to the ground plane of the waveguide. The inner conductor of the shielded stripline is sandwiched in between the two substrates, therefore the parameter d in equation (3.32) is already set and equal to the thickness of the bottom substrate. Looking at equation (3.32) all variables are already set by the predefined circuit parameters except for variable c, the distance the inner conductor is extended into the waveguide. Thus the input impedance seen by the shielded stripline looking into the waveguide can be controlled by varying parameter c. An important parameter that is not defined in equation (3.32) is the radius of the probe. The radius of the via hole has a strong influence on the performance of the transition. The effects of via hole radius is discussed in section 4.4. Figure 3.77 shows both a top view and side view of the

transition.

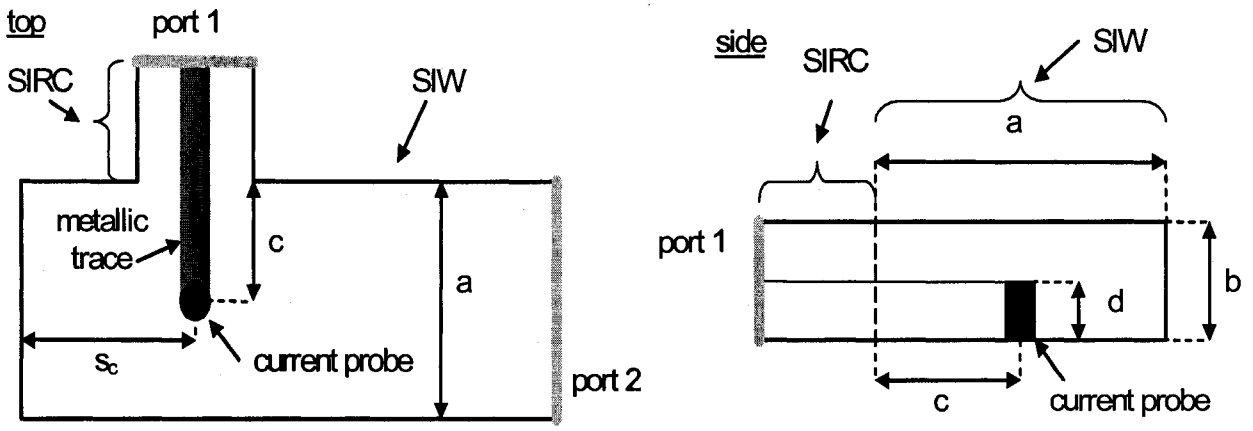

Figure 3.7: A top and side view of the vertical transition between the shielded stripline and SIW [32].

The signal current will flow down the via to the ground plane, this gives rise to a magnetic field that encircles the via. This magnetic field latches onto the waveguide and generates a TE_{10} mode wave that propagates through the waveguide [5,17]. This transformation of the current along the via to the magnetic field in the waveguide is the essence of the transition between the shielded stripline and the waveguide. Figure 3.8 shows the magnetic field generated by the via and how it propagates through the waveguide.

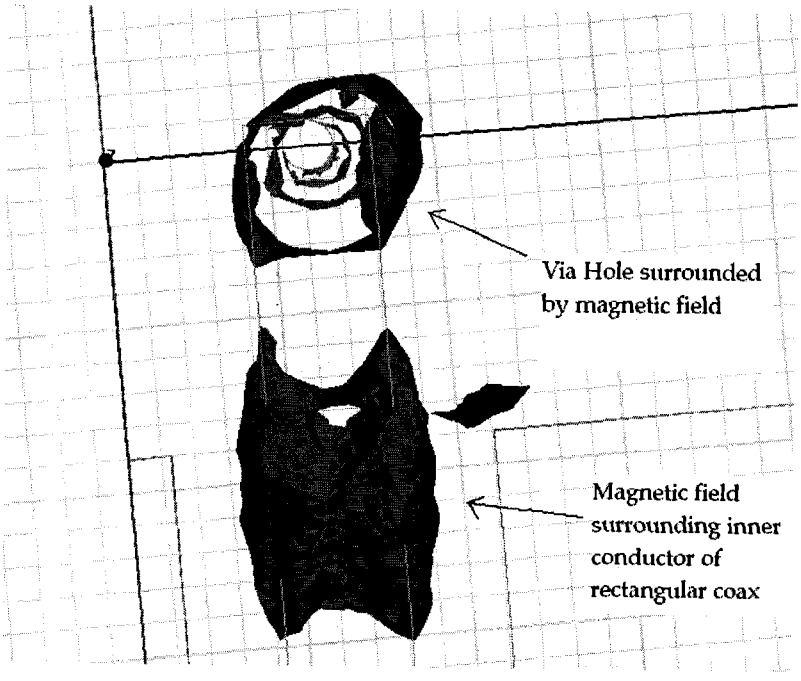

Figure 3.8: Sketch of the magnetic field surrounding the inner conductor of the stripline and the via holed used for the vertical transition.

3.6 Transformation of a Waveguide into an Substrate Integrated Waveguide

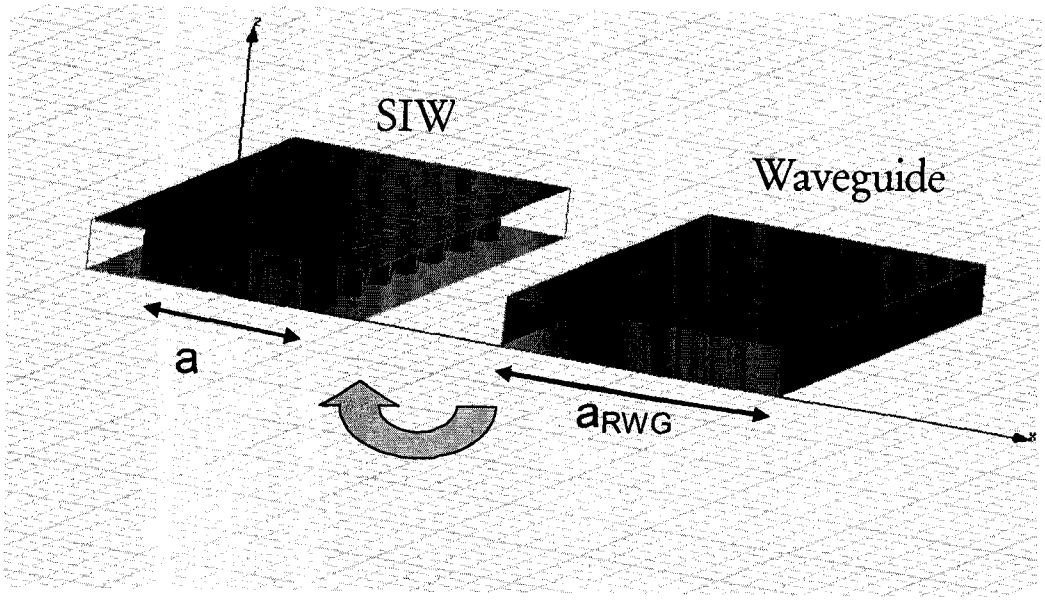

Figure 3.9: Transformation of waveguide to SIW

The theory and design procedure of a slotted, dielectric-filled waveguide antenna and its feeding structure have been presented in the previous sections. This antenna is integrated into a substrate to allow an easy connection between other microwave circuits in the same substrate. A substrate integrated waveguide must be designed in order to replace the dielectric-filled waveguide used for the design of the antenna. The SIW must be equivalent to the dielectric-filled waveguide. The propagation constant and characteristic impedance of the SIW must be the same as the dielectric-filled waveguide. The fundamental difference between the two transmission lines is that the metallic sidewalls of the dielectric-filled waveguide are to be replaced by a row of metallic via holes, one row for each sidewall. Figure 3.10 gives a visual description of the SIW.

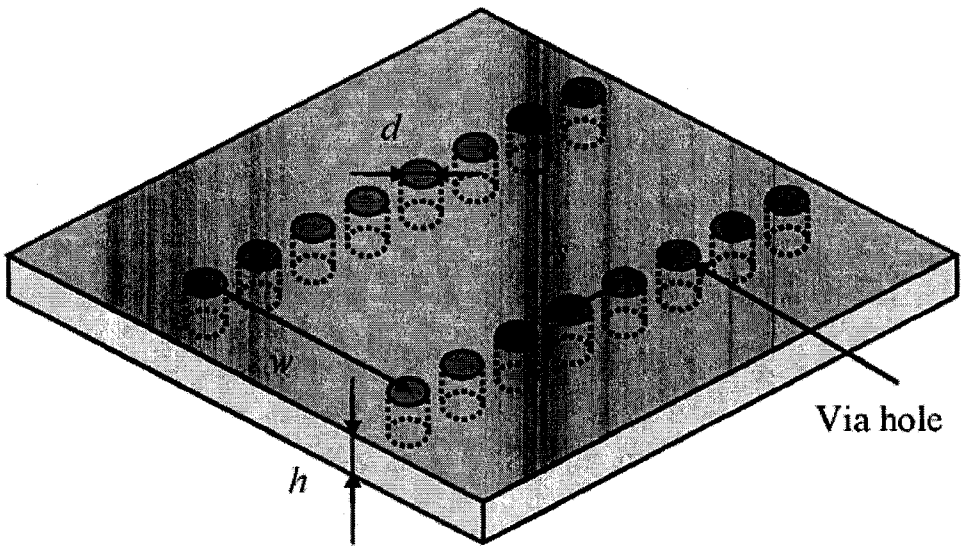

Figure 3.10: Sketch of a substrate integrated waveguide [3].

Referring to figure 3.10 there are two identical rows of via holes which act as a perfect electric conductor along the plane of each row. The two rows of via holes are separated by a distance *a*. Each row is made up of identical via holes that have a diameter *d* and

adjacent vias are separated by a distance *s*. Through careful selection of the parameters *a, s & d,* an SIW can be designed to operate as an equivalent dielectric-filled waveguide with a width a_{RWG} [44,45,46].

Since the sidewalls of the SIW are a linear array of metallic posts, one must be concerned with radiation emanating from in between the posts that results in some wave attenuation due to leakage [1,3,11]. The row of via holes can be viewed as a metallic sidewall with an array of slots cut out of the sidewall [1]. From the theory of slots [7,20-22] discussed in section 3.2, it was stated that when a slot is cut along the direction in which the current is flowing there is very little radiation, however if a slot is cut along the transverse direction of the current then a significant amount of radiation radiates through the slot.

In regular rectangular waveguides different modes have different surface currents associated with them [12]. Figure 3.2 from section 3.2 shows the surface current when the waveguide is excited by a TE_{10} mode wave. The surface currents on the sidewalls travel either up or down the sidewalls of the waveguide, there are not any currents traveling along the longitudinal direction of the waveguide. Therefore if slots are cut out of the sidewalls, there is a small amount of radiation emanating from the slots. However any TM modes or TE_{mn} modes where n is a non-zero number, the surface currents along the sidewalls of the waveguide are not confined to just the up and down direction but to the longitudinal direction as well. This results in a large amount of radiation radiating through the slots. Therefore the SIW is only able to guide TE_{m0} mode waves without incurring a significant amount of leakage through the spaces in between the metallic via holes. For this thesis the slotted waveguide antenna is designed for just the dominant TE_{10} mode and thus a SIW is a suitable choice for the antenna.

Previous work by Wu and Xu [1] have shown that if the metallic posts are not soldered to the ground planes of the substrate, the s-parameters of the SIW degrade significantly. This shows that the posts are not just responsible for containing the electromagnetic fields inside the waveguide, but must also carry the sidewall surface currents in order to preserve the guided wave propagation.

To further study the wave attenuation due to leakage from the gaps in between the posts, one must look at the angle of incidence that the propagating wave inside the SIW reflects off the linear array of posts. Figure 3.11 shows a diagram of how a TE_{10} mode wave propagates through a waveguide.

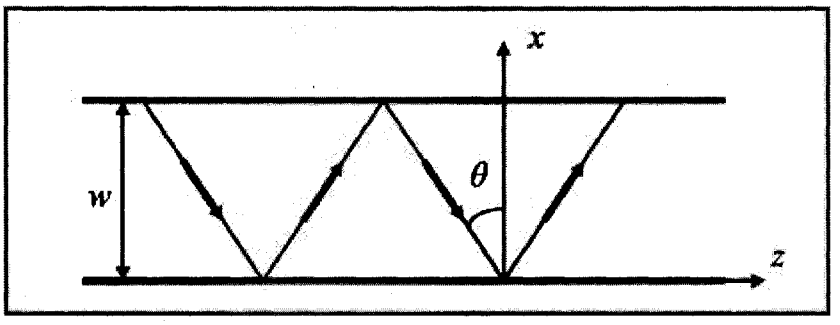

Figure 3.11: TE_{10} mode wave propagating through a waveguide [3].

The angle of incidence can be calculated through the following equation [12]

$$\cos\theta = \frac{m\lambda}{2a} \tag{3.33}$$

Where m is the wave mode number of the TE_{m0} mode, λ is the wavelength, a is the width of the SIW and θ is the angle of incidence. The leakage due to the electromagnetic fields escaping in between the via holes can be approximated through the following equation [1]

$$R_{leak} = 1 - \frac{d}{s\cos\theta} \tag{3.34}$$

Where d is the diameter of the via hole, s is the spacing in between adjacent via holes and θ is the angle of incidence. Figure 3.12 shows a visual description of the electromagnetic waves impinging upon the linear array of via holes.

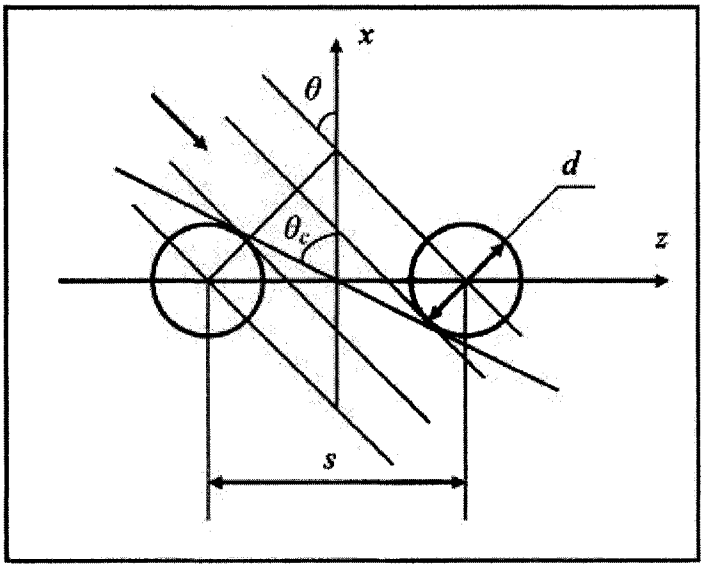

Figure 3.12: Electromagnetic waves in a SIW directed upon 2 adjacent via holes [3].

Looking at equations (3.33 & 3.34) one observes that as the frequency increases while the angle of incidence stays constant, leakage in between the posts increases. However as the frequency increases, the angle will increase as well and thus the leakage will decrease because the angle of incidence has a stronger influence on the leakage characteristic compared to the frequency [3]. The higher the TE_{m0} mode propagating through the SIW, the larger the amount leakage between via holes. Experiments performed by Wu & Xu [3] have proven this to be true. Thus it can be stated that substrate integrated waveguides

are best suited for the propagation of the TE_{10} mode wave. Another important characteristic that will have a significant impact of the leakage of SIW is the ratio of the spacing between adjacent posts and the post's diameter, the *s/d* ratio. Previous work [1,3,11,13] validated through experiments has shown that as the ratio *s/d* increases, so does the wave attenuation due to leakage. The ratio between the width of the SIW and diameter of the post, *d/a,* has an effect on the leakage characteristics as well. Similarly to the *s/d* ratio, experiments [1,3] have verified that as the *d/a* ratio increases so does the leakage. To ensure that the leakage of electromagnetic waves is negligible a condition is set that

$$\frac{s}{d} \leq 2 \tag{3.35}$$

and

$$d \leq 0.2\lambda \tag{3.36}$$

Due to the periodic nature of substrate integrated waveguides, one must be concerned with bandgap effects. When designing an SIW, the designer must ensure that the bandstop is not within the operating frequency band. When dealing with SIW, the bandstop locations are given by the following equation [1]

$$\beta_z s = n\pi \tag{3.37}$$

Where s is the separation distance between adjacent posts and β_z is the phase constant. The first bandstop appears at n=1. From well known microwave theory [12]

$$\beta = \sqrt{k^2 - k_c^2} \tag{3.38}$$

Where k_c is the cutoff frequency wavenumber. When leakage losses are small $k = 2k_c$ and we can rearrange equation (3.38)

$$\beta = \sqrt{4k_c^2 - k_c^2} = \sqrt{3}k_c \tag{3.39}$$

Substituting equation (3.39) into (3.37) gives

$$\frac{s}{\lambda_c} = \frac{1}{2\sqrt{3}} \tag{3.40}$$

Equation (3.38) gives the condition for a bandstop to be located at the end of the waveguide operating bandwidth $k = 2k_c$ which is the cutoff frequency of the TE_{20} mode. In order to ensure that the bandstops are not in the operating bandwidth we can set the condition [1]

$$s \leq 0.25\lambda_c \tag{3.41}$$

Therefore as long as the spacing in between the posts is less than a quarter-wavelength of the cutoff frequency of the TE_{10} mode we can ensure that no bandgaps will be present within the operating bandwidth.

Experiments have shown that if either ratio *s/d* or *d/a* increase then the magnitude of the bandstop along with its bandwidth will increase [3].

This section has discussed the effects of the diameter of the posts and the spacing in between adjacent posts. It is now time to turn towards the third parameter of the SIW, the spacing between the two rows of via holes, *a*. This is essentially the width of the SIW and it is the distance measured from the center to center of the two via holes across from one another, refer to figure 3.10. The parameter *a* must be selected such that the cutoff frequencies of the TE_{10} mode and TE_{20} mode are similar to the cutoff frequencies of the regular rectangular waveguide to ensure that the SIW is able to guide the wave at the proper operating frequency. Cassivi *et al.* [11] have done work on the dispersion properties of SIW. Making use of the BI-RME method and Floquet's theorem Cassivi *et*

al. [11] have derived empirical equations that approximate the cutoff frequencies of the first two dominant modes.

$$f_{c_{TE10}} = \frac{c_0}{2\sqrt{\varepsilon_r}}\left(a - \frac{d^2}{0.95 \cdot s}\right) \tag{3.42}$$

And

$$f_{c_{TE20}} = \frac{c_0}{\sqrt{\varepsilon_r}}\left(a - \frac{d^2}{1.1 \cdot s} - \frac{d^3}{6.6 \cdot s}\right) \tag{3.43}$$

Where a is the SIW width, d is the diameter of the via holes, s is the spacing between adjacent via holes and c_0 is the speed of light. Looking at equation (3.42) one notices that it is very similar to equation for the cutoff frequency of the TE_{10} mode in a rectangular waveguide, equation (4.1). The only difference is that width of the rectangular waveguide, a_{RWG}, is replaced by the term in the brackets. This demonstrates the relationship between the rectangular waveguide width and the SIW width for this particular empirical equation.

$$a_{RWG} = a - \frac{d^2}{0.95 \cdot s} \tag{3.44}$$

There exists a more accurate method [3] for determining the equivalent rectangular waveguide width of a SIW. This method calculates the propagation constant of the SIW and in turn uses that information to derive the equivalent width of a rectangular waveguide. To determine the propagation constant two sections of the SIW of different lengths L_1 & L_2 are simulated with the software package HFSS. Since the two SIW sections are identical, except for their lengths, they will have the same propagation constant. However because of the difference in lengths, the phase at the end of the transmission line will be different from each other. The phase difference and length of the

two SIW are known and that information can be used to calculate the propagation constant of the SIW with the following equation

$$\beta_{SIW} = \frac{\angle S_{21}^{L2} - \angle S_{21}^{L1}}{L_1 - L_2} \tag{3.45}$$

Once the propagation constant is determined the equivalent rectangular waveguide width can be calculated with the following equation

$$a_{RWG} = \frac{\pi}{\sqrt{\omega^2 \mu_0 \varepsilon_0 \varepsilon_r - \beta_{SIW}^2}} \tag{3.46}$$

3.7 Transformation of a Rectangular Coax to a Shielded Stripline

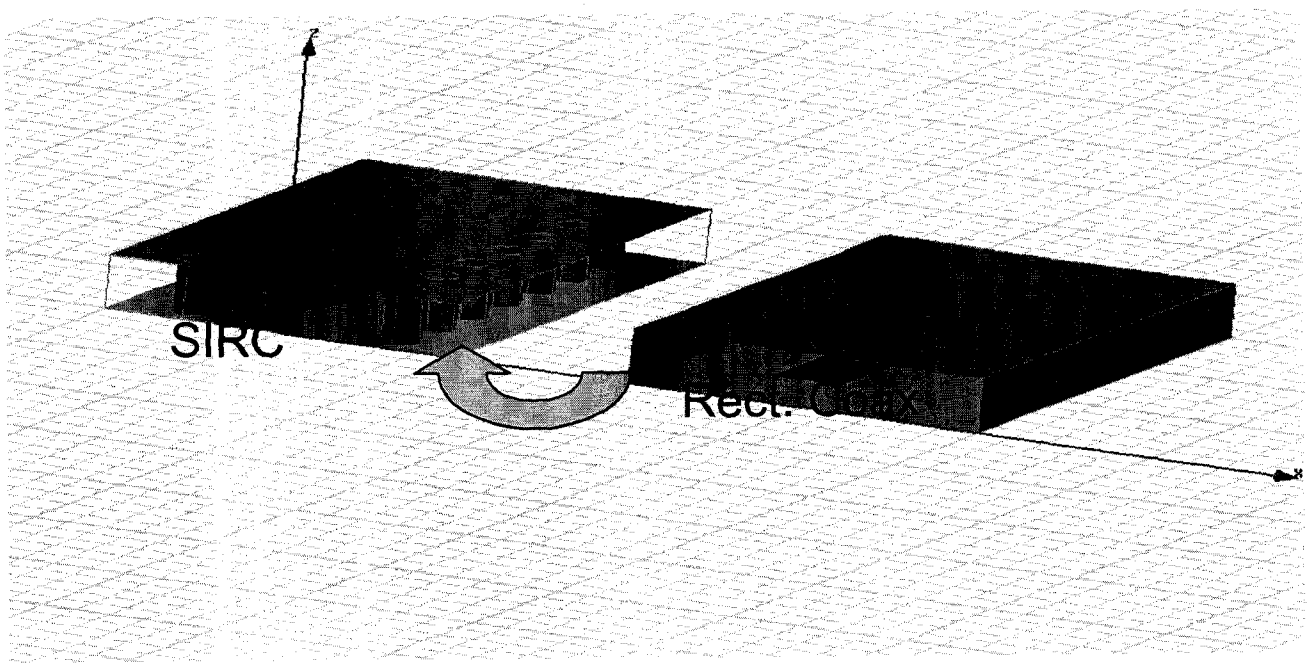

Figure 3.13: Transformation between a rectangular coax and a shielded stripline or a substrate integrated rectangular coax (SIRC).

The SIW antenna was initially fed with a rectangular coax. The design equations for the

rectangular coax are given in section 3.5. Since the antenna itself is integrated in the substrate, the fed network must also be integrated in the substrate. This is a very similar problem to the transformation of a waveguide to an SIW. The designer is to replace the sidewalls of the rectangular coax with two rows of metallic via holes. A top view diagram of the shielded stripline is given in figure 3.14.

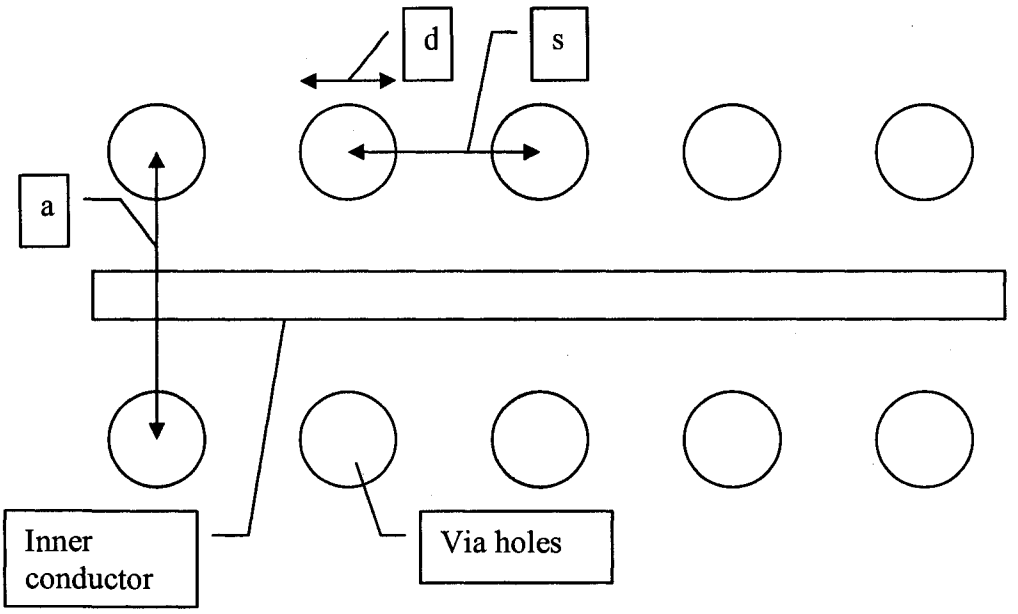

Figure 3.14: Top view of shielded stripline.

Just as in the SIW case we have three parameters which dictate the geometry of the via holes, the post diameter *d,* the spacing between adjacent post *s* and the distance between the two rows *a*. Much of the theory of section 3.6 can be applied here. The *s/d* ratio must be kept small enough so that most of the electromagnetic fields are contained within the two rows of vias. The distance between the two rows must be carefully chosen so that the shielded stripline has the same characteristic impedance and propagation constant as the rectangular coax.

Chapter 4

Results

4.1 Introduction

This chapter begins with the characterization of an isolated slot cut out of a waveguide. Characterizing the impedance properties of an isolated slot is the first step in designing a slotted waveguide. The admittance properties of an isolated slot as a function of length and offset $Y/G_0(x_n, l_n)$ is characterized with the use of the high frequency software package HFSS from Ansoft. HFSS utilizes the finite element method to numerically solve Maxwell's equations. For all HFSS simulations an adaptive meshing scheme was used. The adaptive meshing constructs a mesh that conforms to the electrical performance of the device. The mesh is automatically tuned to give the most accurate and efficient mesh possible. In general the mesh is sized to a quarter of a wavelength for air and one third of a wavelength for dielectrics. After each adaptive pass the S-parameters of the current mesh are compared to the previous mesh, if the solution has changed by less than the convergence value then the solution is said to be converged. The convergence value is set to 0.02 (2%). Using the design procedure detailed in chapter 3 a slotted waveguide antenna array is designed and simulated. The second part of this chapter deals with the design of a vertical transition between a stripline and waveguide. The transition is based upon Harrington's [17] model of a transition between a coaxial cable and a waveguide which has a very similar geometry to the vertical transition between a stripline and waveguide. A transition between a microstrip line and a rectangular coaxial cable is then designed with the goal of minimizing mismatch between the two transmission lines and the complexity of the transition by keeping the transition

planar. The final part of this chapter deals with transforming the rectangular waveguide into an equivalent substrate integrated waveguide which has the same wave propagation and frequency cut-off properties as the rectangular waveguide. The same transformation must be done to the rectangular coaxial creating a substrate integrated rectangular coax.

4.2 Validation of Methodology of Slot Characterization

In section 3.4 & 4.3 of this thesis we discuss the methodology of characterizing an isolated slot in a waveguide as well as show its results. To validate this methodology we have followed the same procedure for the slot characterization of an air-filled waveguide with dimensions $a=0.9in$, $b=0.4in$ and slot width $w=1.3875mm$ at a frequency of $f=9.375GHz$ and compared the results with previously published results of an isolated slot with the same dimensions. The curve describing the relationship between the resonant length of a slot and its offset is validated by comparing the results to those found by Josefsson [19].

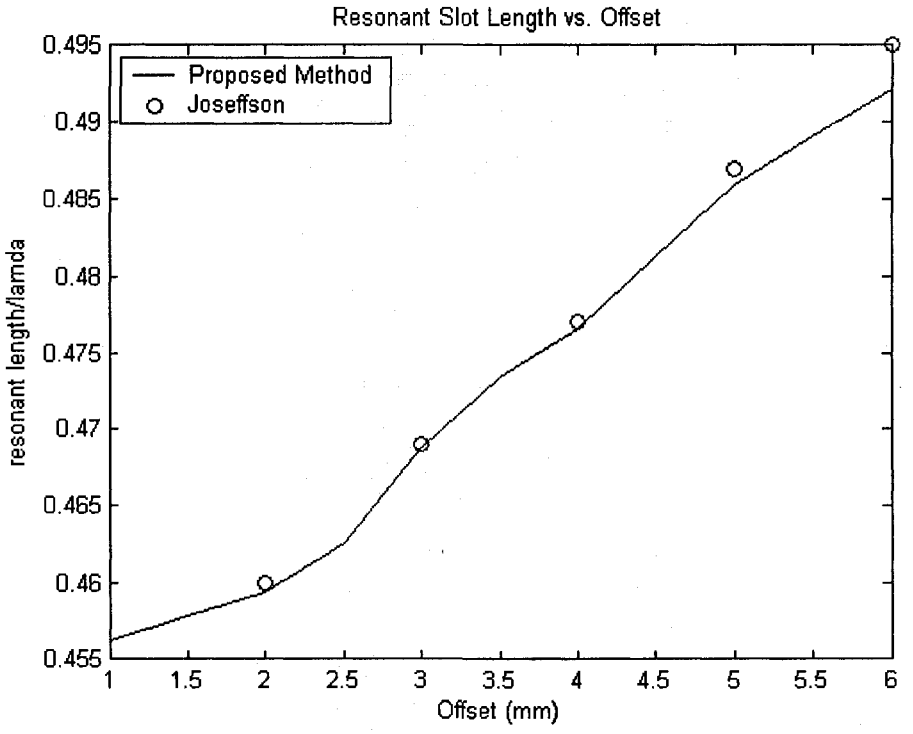

Figure 4.1: Comparison between Joseffson's [19] results and the proposed slot characterization method.

Analyzing figure 4.1 shows that proposed slot characterization method gives similar results when compared to Josefsson's [19] data. Only when the offset reaches 6mm is difference noticed. A 6mm offset is a rather large offset and for this thesis the slots displacement from the centerline will be considerably smaller than 6mm.

The curve that displays the normalized conductance with respect to the offset is validated by comparing it with Stevenson's [48] formula for a slot in a waveguide.

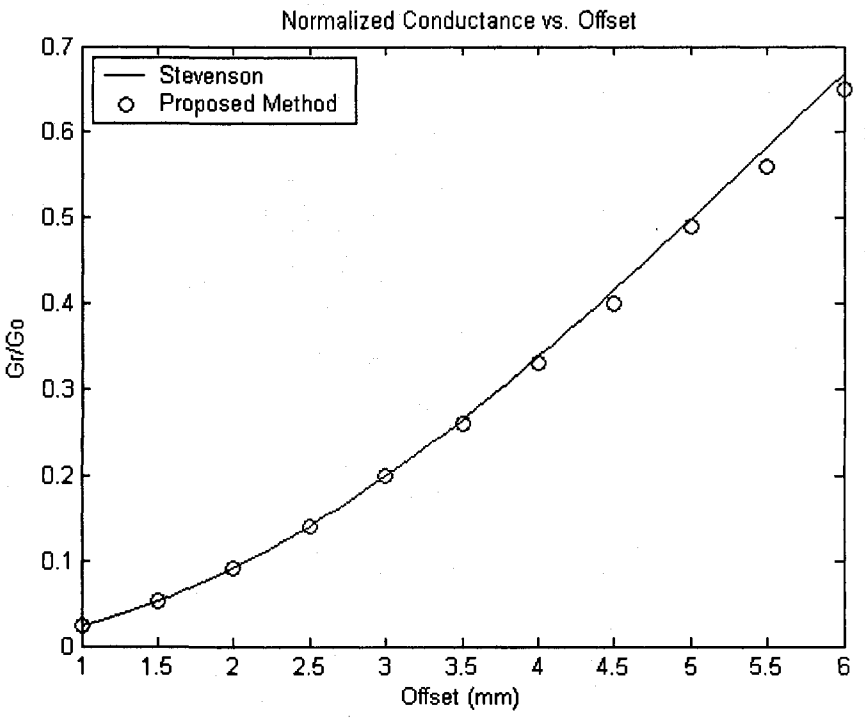

Figure 4.2: Comparison between Stevenson's [48] formula for resonant conductance and proposed slot characterization method.

Looking at figure 4.2 we see excellent agreement between the proposed method and Stevenson's [48] formula for slot conductance.

$$\frac{G}{G_0} = \left[2.09 \frac{\lambda_g}{\lambda_0} \frac{a}{b} \cos^2\left(\frac{\pi \lambda_0}{2\lambda g} \right) \right] \cdot \sin^2\left(\frac{\pi x}{a} \right) \tag{4.1}$$

Stevenson's [48] formula shows good results so long as the slots are resonant. If the slots are not at resonant length the formulas accuracy begins to deteriorate. For this reason we are only using Stevenson's [48] formula to validate the resonant slot length vs. offset curve. The impedance of the slot determined through the proposed method is compared to Khac's [49] data.

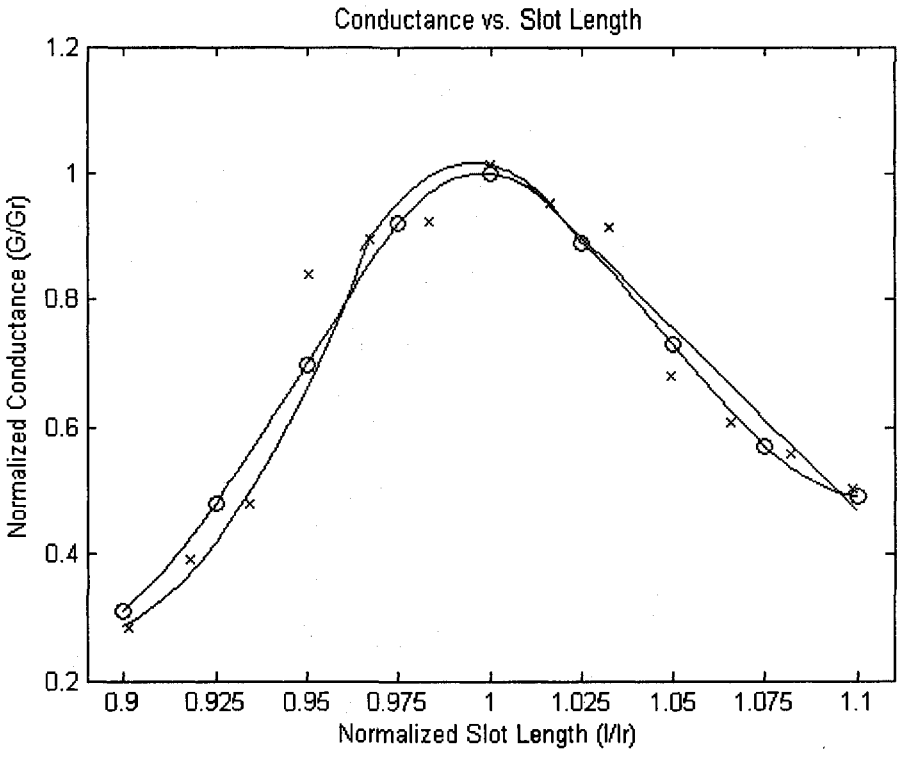

Figure 4.3: Comparison between Khac's [49] data on the slot conductance and proposed method.

Analyzing both figure 4.3 & 4.4 one sees that the data accumulated through the proposed method of the slot's impedance properties shows good agreement with Khac's and Carson's [49] work on the impedance properties of an isolated slot. These results instill confidence in the proposed method that determines the impedance properties of an isolated slot, which is a crucial design step in designing a slotted waveguide antenna.

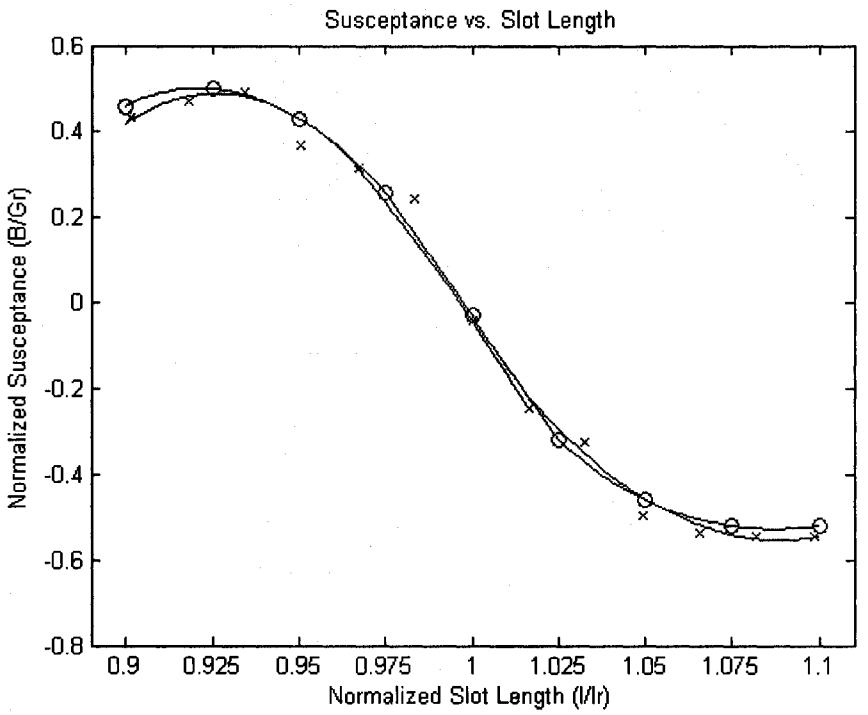

Figure 4.4: Comparison between Khac's [49] data on the slot susceptance and the proposed method.

4.3 Characterization of an Isolated Slot in a Waveguide

The goal of this section is to determine the admittance properties of a slot cut out of a waveguide. The design frequency of the antenna was chosen to be 15GHz. It is desired to have only the TE_{10} mode wave propagating through the waveguide, all other higher order modes must be attenuated to a negligible quantity. This can easily be achieved by choosing appropriate waveguide dimensions. The ultimate goal is to integrate the waveguide into a planar circuit so that the antenna can be easily integrated with other microwave circuits in the same substrate. Due to fabrication limitations of such circuits as well as predefined circuit parameters of the substrate it is imperative that the *b* dimension of the waveguide equal 60mil. The substrate that is used for this circuit has been

predefined to be Rogers Duroid 6002 which has a dielectric permittivity of $\varepsilon_r = 2.94$. With these conditions already in place the only dimension of the waveguide of which the designer has control is the width of the waveguide, dimension *a*. Fortunately it is this dimension which controls the cutoff frequency of the dominant TE_{10} mode through the following equation [12]

$$f_{c10} = \frac{1}{2a\sqrt{\mu\varepsilon}} \tag{4.1}$$

The first higher order mode of the waveguide, the TE_{20} mode must not be allowed to propagate through the waveguide. Therefore dimension *a* must be chosen so that the design frequency is above the cutoff frequency of the TE_{10} mode, f_{c10}, yet below the cutoff frequency of the TE_{20} mode, f_{c20}. The cutoff frequency of the TE_{20} mode can be found with the equation

$$f_{c20} = \frac{1}{a\sqrt{\mu\varepsilon}} \tag{4.2}$$

Choosing $a=9mm$ corresponds to $f_{c10}=9.71GHz$ and $f_{c20}=19.43GHz$. This *a* dimension will allow the TE_{10} mode wave to freely propagate through the dielectric-filled waveguide while all other higher order modes will decay exponentially from the source at the design frequency of 15GHz and dielectric permittivity of $\varepsilon_r=2.94$.

Now that we have the appropriate waveguide dimensions, the admittance properties of a slot cut out of this specific waveguide can be determined. In chapter 3 it was discussed that when a TE_{10} mode wave is propagating through a waveguide, which has a slot cut out from it, the voltage induced in the slot is symmetrical and thus the slot can be represented by a lumped shunt admittance at the center of the slot [7,20-22]. Since the

slot can be viewed as a shunt admittance, the admittance properties of the slot can be easily calculated with the use of equation (3.26). In order to determine the scattering matrix of the slot a commercial computer program Ansoft HFSS was used to model the slotted waveguide. The model consisted of a section of the specific waveguide described above with a length of λ_g. The slot was cut out of the middle of the waveguide and the waveguide was terminated with an absorbing boundary condition.

Simulations were performed by varying the length of the slot from $0.9l_r < l < 1.1l_r$ while keeping the offset constant. These simulations were repeated for different offsets varying between 10mils to 40mils at 5mil intervals. It is first necessary to find the resonant length of the slot at different offsets. For regular rectangular waveguides the resonant length is usually around $\lambda_g/2$. However because the b dimension of the dielectric-filled waveguide we are studying is considerably smaller than regular manufactured rectangular waveguides, the resonant length of the slot is substantially longer. Figure 4.5 shows how the resonant length of the slot varies with respect to the slot offset from the centerline of the waveguide.

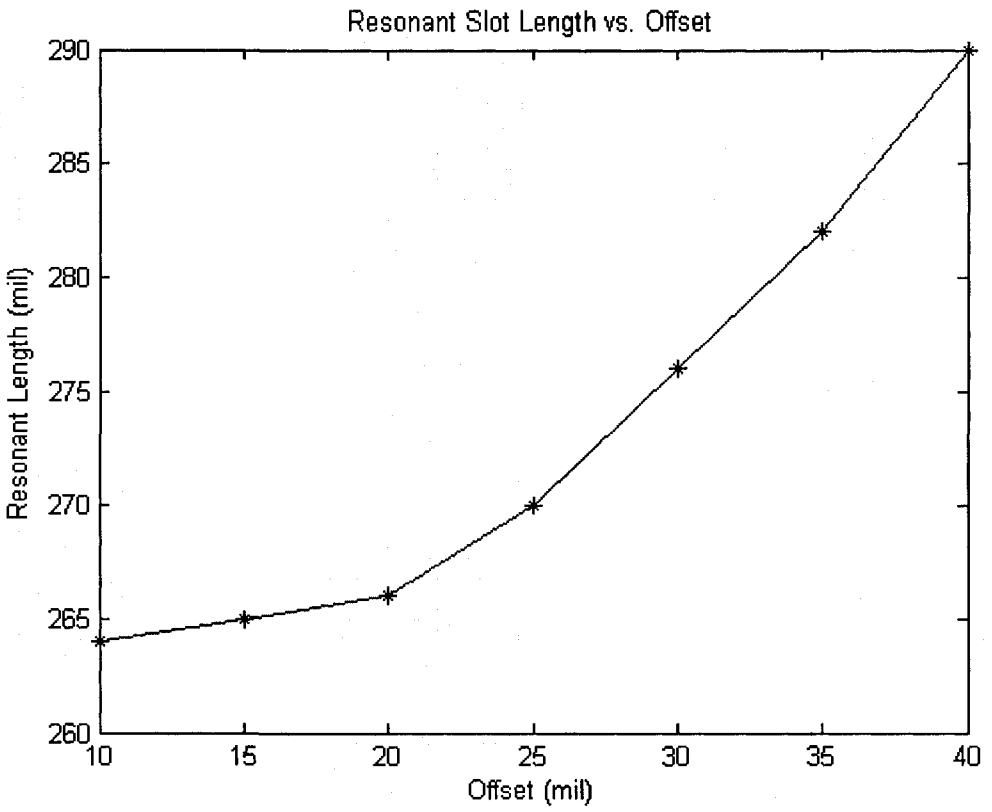

Figure 4.5: Resonant slot length with respect to offset.

For each offset, 10-40mil in steps of 5mil, the length of the slot is varied around the resonant length. The real and imaginary part of the slot's self-admittance has been plotted. The resonant length is the length in which the reactance is zero. A plot of the self-admittance curves for an offset of 30mil is given in figure 4.6.

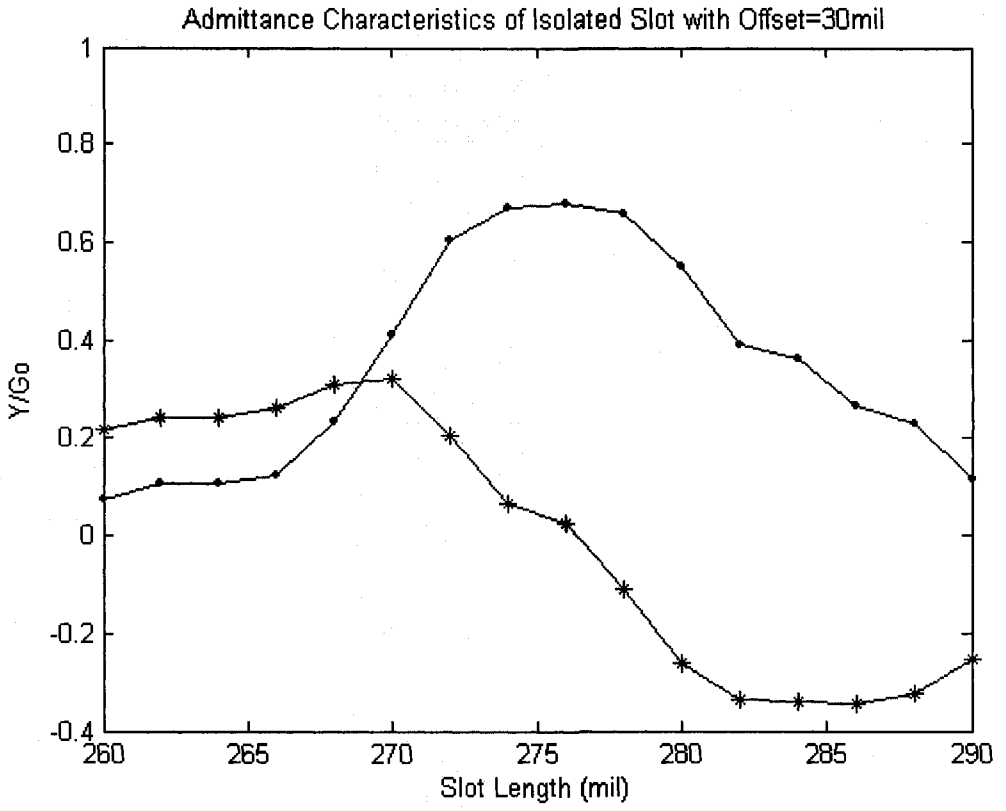

Figure 4.6: Self-admittance curve for an offset of 30mil.

Similar curves were obtained for the other offsets. A general trend that is apparent when analyzing these curves is that the admittance increase as the offset increases, however the envelopes of the curves were very similar for different offsets. This trend was predicted by previous work on slotted waveguides [7]. If all curves are divided by their respective resonant conductance, G_r, the plots for each offset will be very similar. Since these plots are alike one can choose one of them, find poly-fitting equations to the real and imaginary curves, and use those equations to design a slotted waveguide. The resonant conductance with respect to the offset is plotted in figure 4.7.

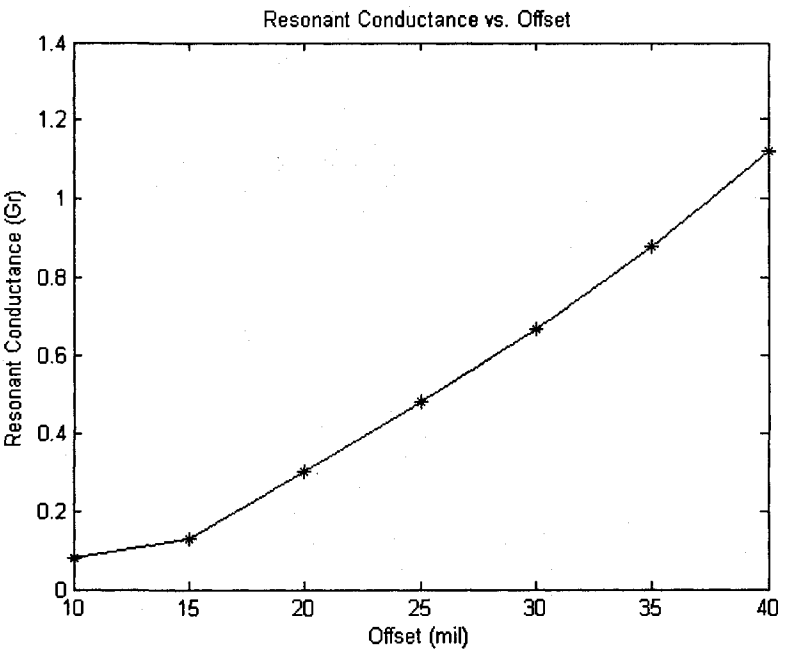

Figure 4.7: The resonant conductance of a slot for different offsets.

The poly-fitted data of the conductance for an offset of 30mil is given in figure 4.8.

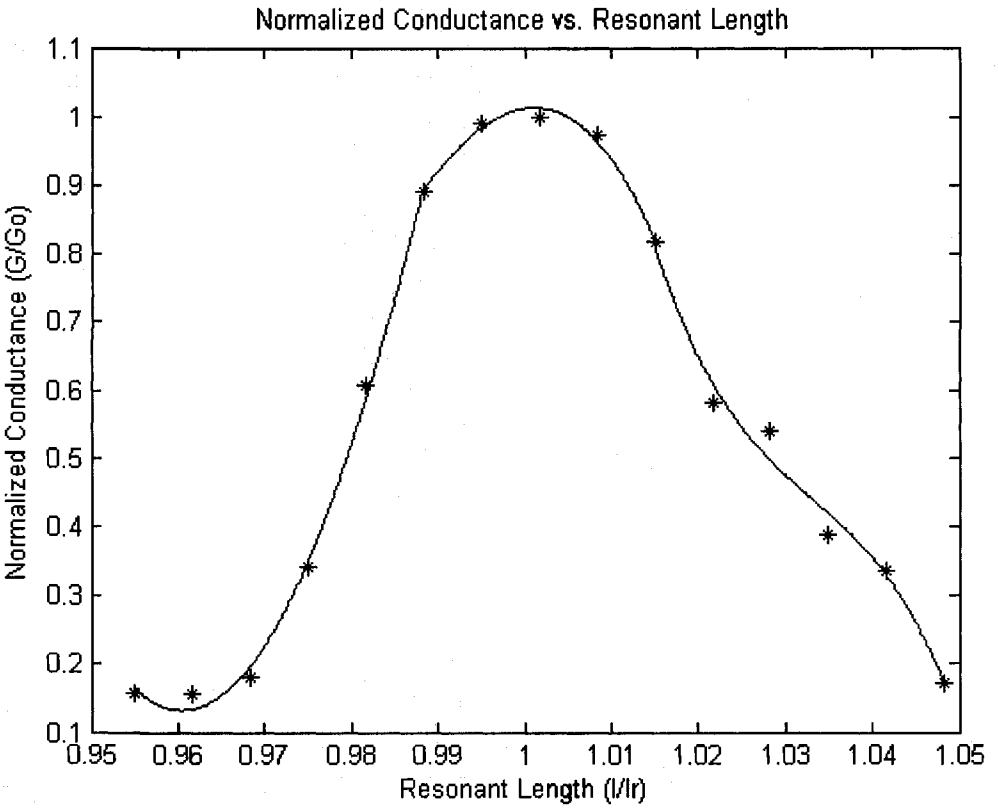

Figure 4.8: Poly-fitted data of conductance for a 30mil offset.

The poly-fitted data of the susceptance of the slot for a 30mil offset is plotted in figure 4.9.

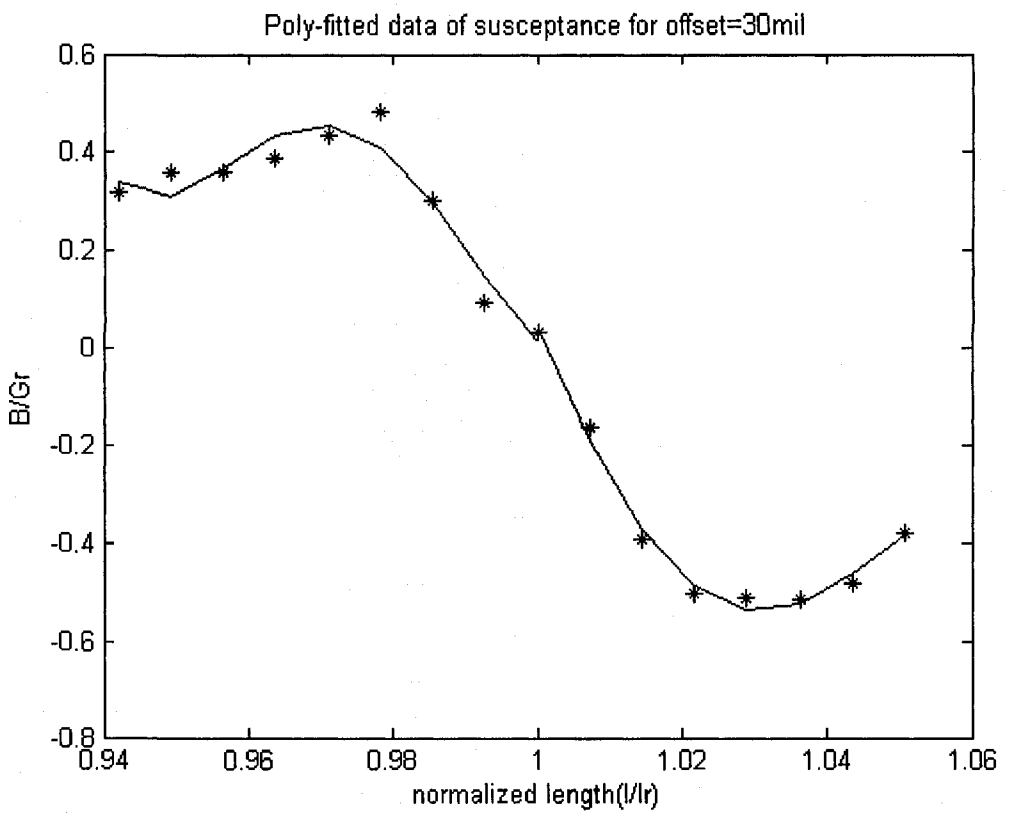

Figure 4.9: Poly-fitted data of the slot susceptance for a 30mil offset.

The polynomial equations of the conductance and susceptance are used to search for appropriate offsets and lengths according to the design procedure discussed in section 3.4.

4.4 Slotted Waveguide Antenna

There are many applications where an antenna is needed to have a high directivity. The directivity of an antenna can be increased, by increasing the electrical size of the antenna itself [25]. This can be accomplished by adding multiple radiating elements to the antenna. For a slotted waveguide antenna one can design a linear array of slots cut out of a single waveguide or a two-dimensional array of slots which consists of multiple linear

arrays of slotted waveguides placed side by side of each other. The larger the number of elements, the higher the directivity of the antenna. The designer can also squint the main beam in a desired direction by appropriately controlling the phase of each slot [25].

In the previous section the admittance properties of an isolated slot was determined. Using this information and following the procedure described in section 3.4 a slotted waveguide antenna can be designed. For this thesis a linear resonant array of 8 slots of uniform amplitude was designed. Figure 4.10 shows a sketch of the slotted waveguide that was designed and just below it figure 4.11 gives the equivalent circuit of slotted waveguide antenna.

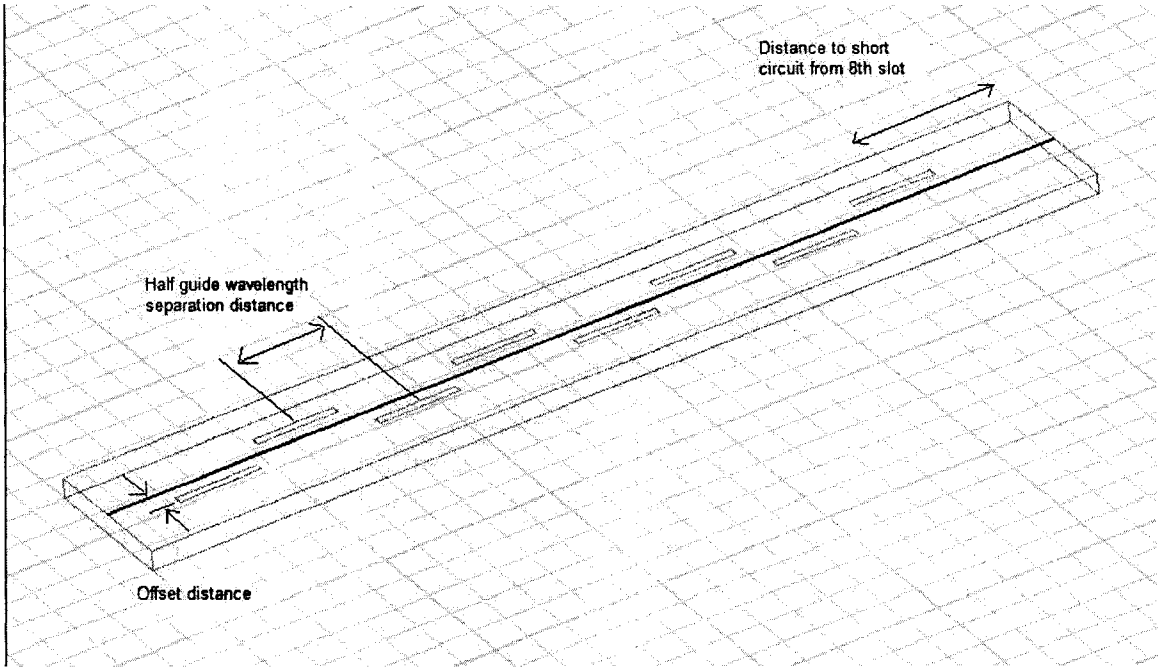

Figure 4.10: Slotted waveguide antenna with 8 longitudinal slots.

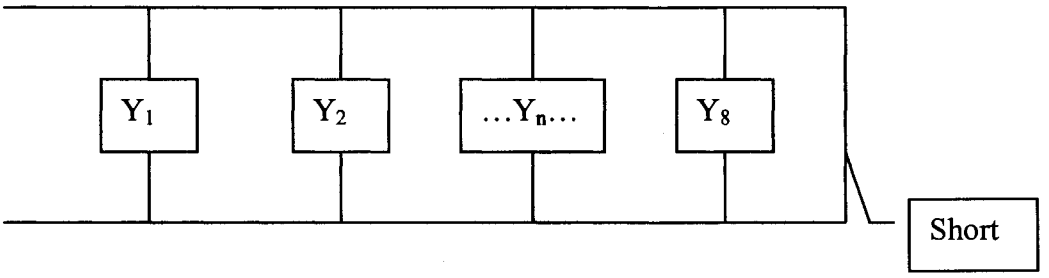

Figure 4.11: Equivalent circuit of a resonant array of slots in a waveguide.

The slots are resonantly spaced apart by a distance of $\lambda_g/2$ and the waveguide is terminated with a short circuit by a distance of $3\lambda_g/4$ from the final slot. Since the slots are spaced apart by $\lambda_g/2$ the phase of each adjacent slot will differ by 180°. The phase difference is compensated for by alternatively placing adjacent slots on the opposite side of the waveguide centerline, refer to figure 4.10. Looking at equation (3.10) one notices that this alternative slot placement cancels out the 180° phase shift. Therefore the phase of the slot voltage in each slot is the same [7,8]. This configuration ensures a resonant antenna with a main beam positioned in the broadside direction. The power distribution to the individual slots must be uniform, this will allow the antenna to have a large directivity, although the sidelobes will be about 13.5dB below the main beam. To ensure a uniform distribution of power the amplitude of the slot voltage must be the same for all slots [25]. Figure 4.7 shows that each slot has its own admittance. By carefully choosing the offset and length of the slot one can control the admittance of each slot and at the same time control the amplitude of the slot voltage. Each slot appears in parallel with each other thus to get a good match the sum of the admittances of the slots must equal the

characteristic admittance of the waveguide at the design frequency of 15GHz. Following the procedure in section 3.4 along with the data found in section 4.2 a uniform array of 8 longitudinal slots in a dielectric-filled waveguide has been designed and simulated with the software package HFSS. The design parameters of the slotted waveguide are as follows

Antenna Dimension	**Offset**	**Length**
Slot #1	17mil	242mil
Slot #2	21mil	245mil
Slot #3	21mil	245mil
Slot #4	17mil	242mil
Slot #5	17mil	242mil
Slot #6	21mil	245mil
Slot #7	21mil	245mil
Slot #8	17mil	242mil
Short circuit distance	450mil	
Slot Width	22mil	
Guide Wavelength	602mil	

Table 4.1: Slotted Waveguide Dimensions.

Figure 4.12 shows the E-plane radiation pattern of the antenna. From the radiation pattern the half-power beamwidth of the antenna was calculated to be 17°. The two main sidelobes of the antenna can be found at $\theta=\pm 29°$, their peaks are both 13.5dB below the

main beam.

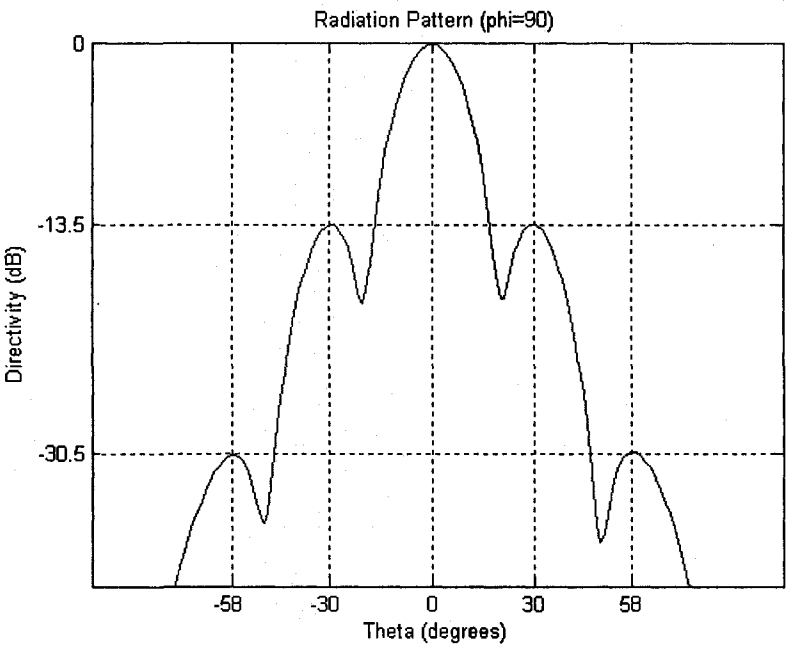

Figure 4.12: E-plane radiation pattern.

Figure 4.13 shows the H-plane radiation pattern. In this plane the radiation pattern is one of a single slot due to the linear nature of the array.

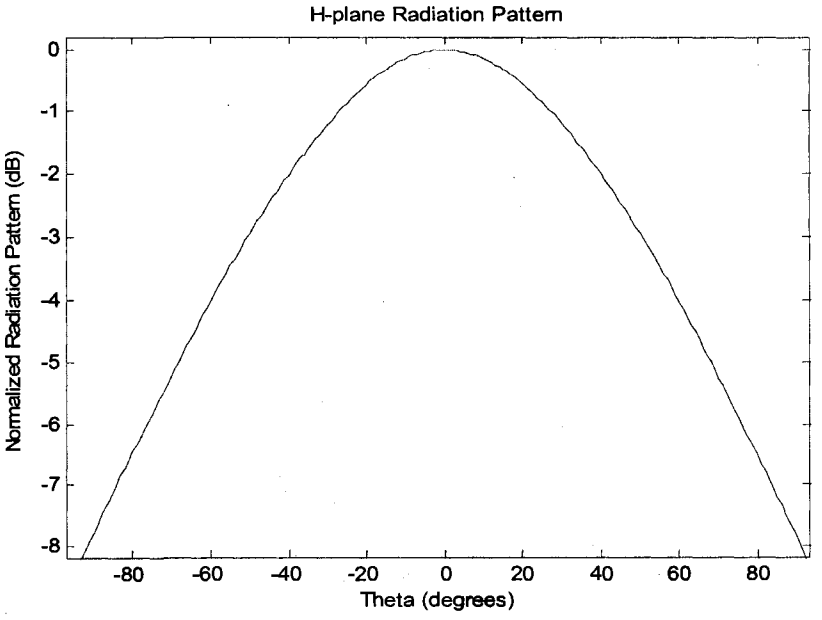

Figure 4.13: H-plane radiation pattern.

The dimensions of the waveguide and slots were carefully chosen to give a good impedance matching at the design frequency of 15GHz. Since the physical dimensions of the slots determine the resonating frequency and of course the slot dimension cannot be changed, the slotted waveguide antenna has the characteristic of a narrow frequency band. As the frequency moves away from the design frequency the impedance match begins to deteriorate. Figure 4.14 shows the return loss of the slotted waveguide antenna. The bandwidth of the antenna for a return loss of less -10dB was measured to be 900MHz which gives the antenna a 6% bandwidth. Modifying the offsets and lengths can increase the antenna's bandwidth, using a non-resonant array of slots can significantly increase the antenna's bandwidth however in both cases the radiation pattern is degraded.

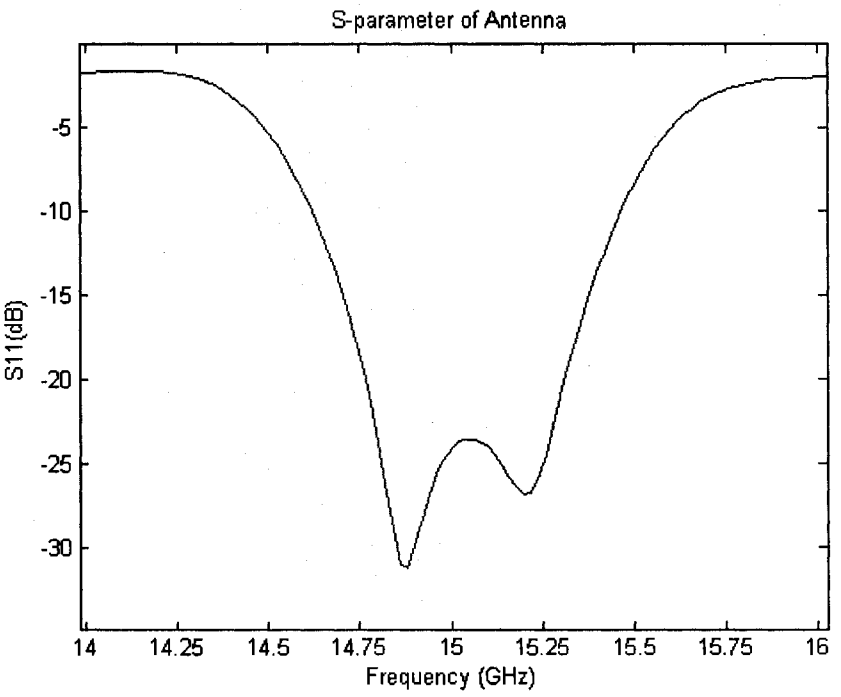

Figure 4.14: Return loss of the slotted waveguide antenna.

4.5 Vertical Transition between Rectangular Coax and Waveguide

In the previous section a slotted waveguide antenna was designed and simulated. However the simulations were conducted with the waveguide being fed by a wave port. The wave port essentially stimulates a TE_{10} mode wave that propagates through the waveguide. Such imaginary wave ports cannot be realized in the real world and thus a feeding scheme must be devised. The waveguide antenna will be fed with a shielded stripline. A metallic via hole will connect the inner conductor of the stripline to the waveguide.

First a rectangular coax must be designed to have a characteristic impedance of 50Ω. Through the use of equations (3.29-3.31) the dimensions of the rectangular coax were calculated to achieve a characteristic impedance of 50Ω. The dimensions are as follows

Rectangular Coax Dimensions	**Numerical Value**
Dielectric Constant, ε_r	2.94
Inner Conductor Width, w_i	40mil
Inner Conductor Thickness, t	0mil
Outer Conductor Width, w_o	185mil
Outer Conductor Height, d	60mil

Table 4.2: Rectangular Coax Line Dimensions.

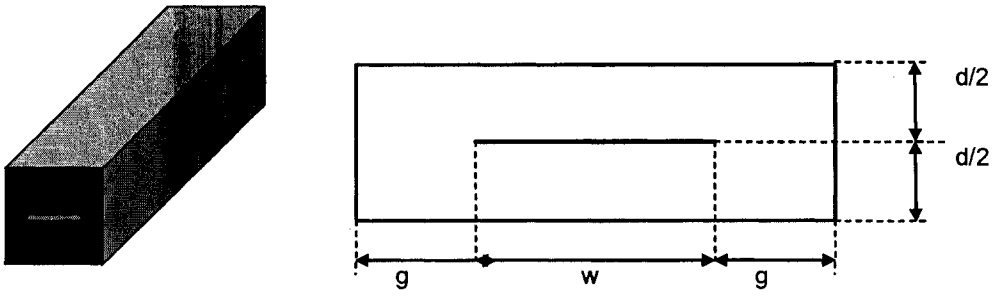

Figure 4.15: Diagram of rectangular coax [32].

The rectangular coax was simulated with HFSS using the dimensions in table 4.2. A wave port with a characteristic impedance of 50Ω was used to excite the transmission line. The S-parameters show how well the rectangular coax is matched to a 50Ω line.

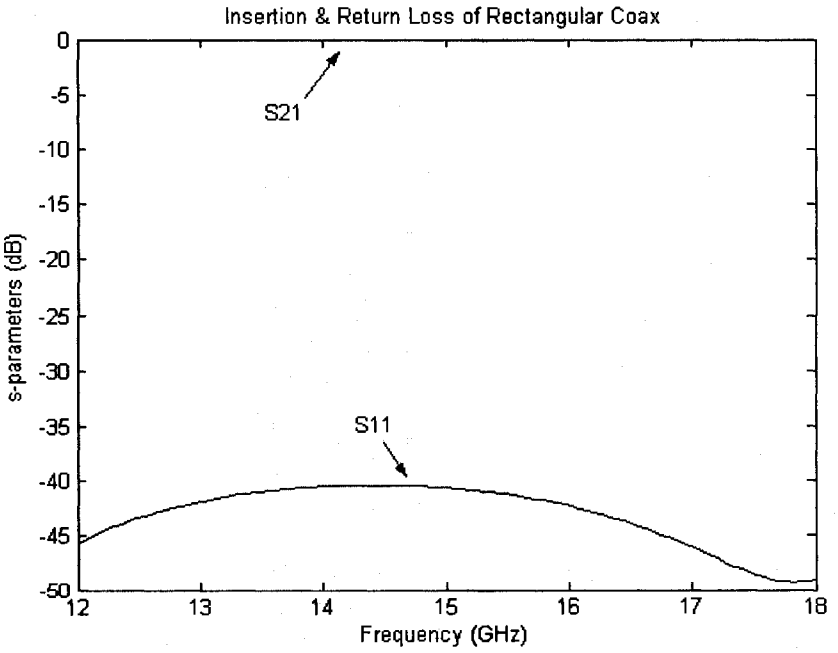

Figure 4.16: Insertion Loss & Return Loss of Rectangular Coax.

Looking at the S_{11} curve in figure 4.16 the results show a good match to the 50Ω line. The bandwidth of the transmission line is also very large. This is due to the geometry of the rectangular line. The electromagnetic fields propagating along the rectangular line are very similar to those of a stripline [31]. Thus a quasi-TEM mode wave propagates along the rectangular line which gives rise to a large bandwidth.

The dimensions of the waveguide have already been calculated in section 4.2, where $a=9mm$ and $b=1.524mm$. The inner conductor of the rectangular coax will extend into the waveguide through an opening in the side of the waveguide as shown in figure 3.7. The two parameters left to calculate are the distance the inner conductor extends into the waveguide, parameter c, and the radius of the via hole that connects the inner conductor to the ground plane of the waveguide. With the use of equation (3.32) the parameter c can be calculated. There is more than one solution to equation (3.32). Using the computer program MATLAB a number of solutions can be plotted to see how the impedance characteristics change with frequency. Figure 4.13 shows a plot of two solutions to equation (3.32).

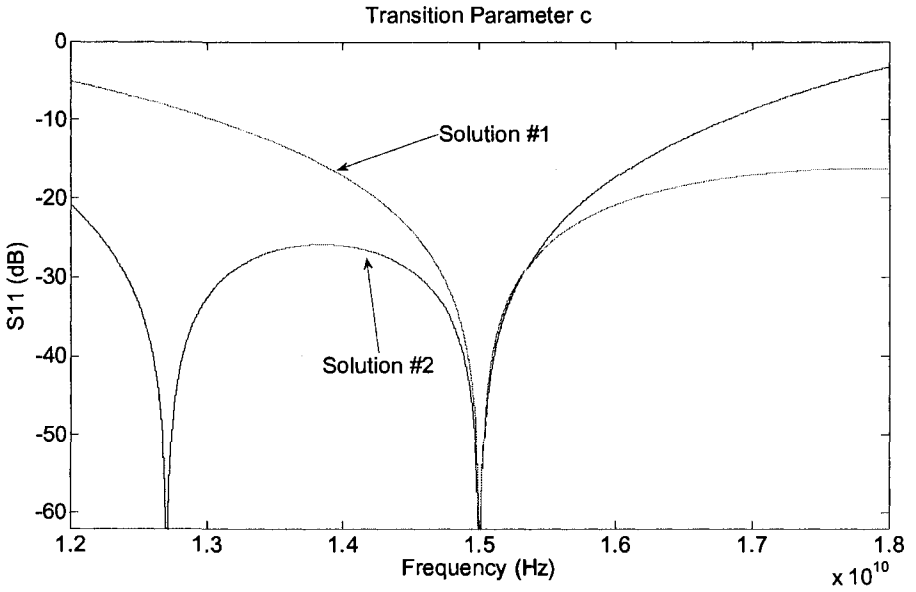

Figure 4.17: Solutions to equation (3.32).

Figure 4.17 gives an idea of how the impedance matching to 50Ω varies with frequency. Notice that at 15GHz there is a notch which shows that according to equation (3.32) the line is perfectly matched to 50Ω.

The final parameter that must be found is the radius of the via. This via hole is the essence of the transition since the current traveling down the via cause a magnetic field to surround the via and in turn create a TE_{10} mode wave that propagates through the waveguide [5,17]. The s-parameters of the transition are rather sensitive to the radius of the via hole. Simulations of the transition are performed with the commercial software package HFSS. These simulations are used to find the appropriate radius of the via which will give the best return loss. The simulations used two wave ports. One wave port feeds the shielded stripline and has a characteristic impedance of 50Ω and another at the end of the waveguide that is perfectly matched to the waveguide. These simulations are performed for different values of the via radius. A plot of how the S11 parameter varies

with the via hole radius is given in figure 4.18.

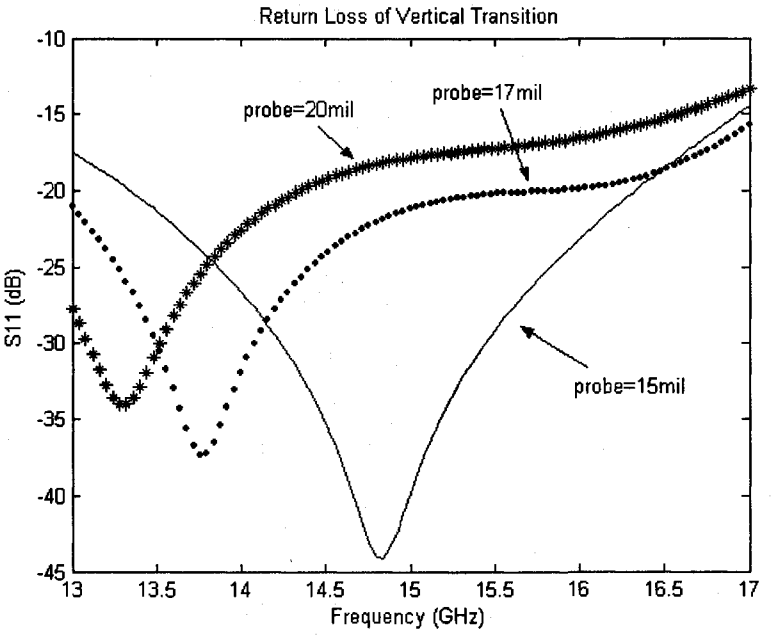

Figure 4.18: The effect on the return loss of the transition as the radius of the probe is varied. Transition designed for Ku band frequency operation.

Reviewing figure 4.18 shows the clear dependence the transition has on the via radius. It is also interesting to see the how the performance of the transition changes when the height of the waveguide, dimension *b*, is varied. Since the waveguide height is varied the length of the probe must vary with the waveguide, this is due to the fact that the probe length is set to *b/2*. Figure 4.19 shows how the impedance matching performance of the transition changes when the height of the waveguide is varied between 60mil to 120mil in steps of 30mil. The results clearly show that as the waveguide height is increased the performance of the transition is improved. It should be noted that the probe diameter was kept constant at 15mil.

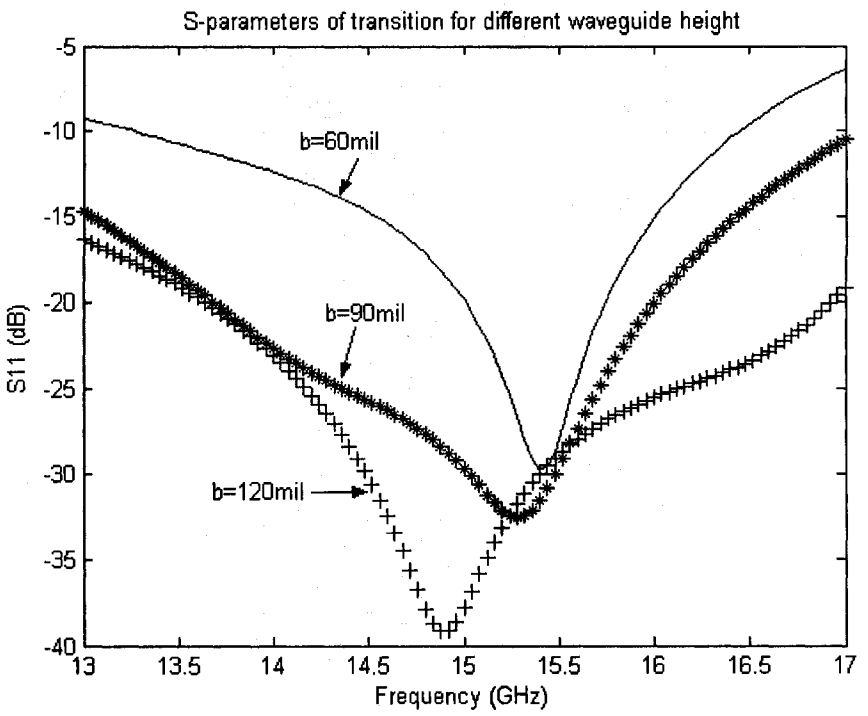

Figure 4.19: Return loss of transition as waveguide height is varied.

To completely test the transition the metallic sidewalls of the shielded stripline and waveguide were replaced with metallic via holes following the procedure describe in sections 3.6 & 4.5 turning the design into a viable substrate integrated circuit. Three back-to-back transitions were designed and simulated for the C band, Ku band and Ka band. A diagram of the back-to-back transition is given in figure 4.20.

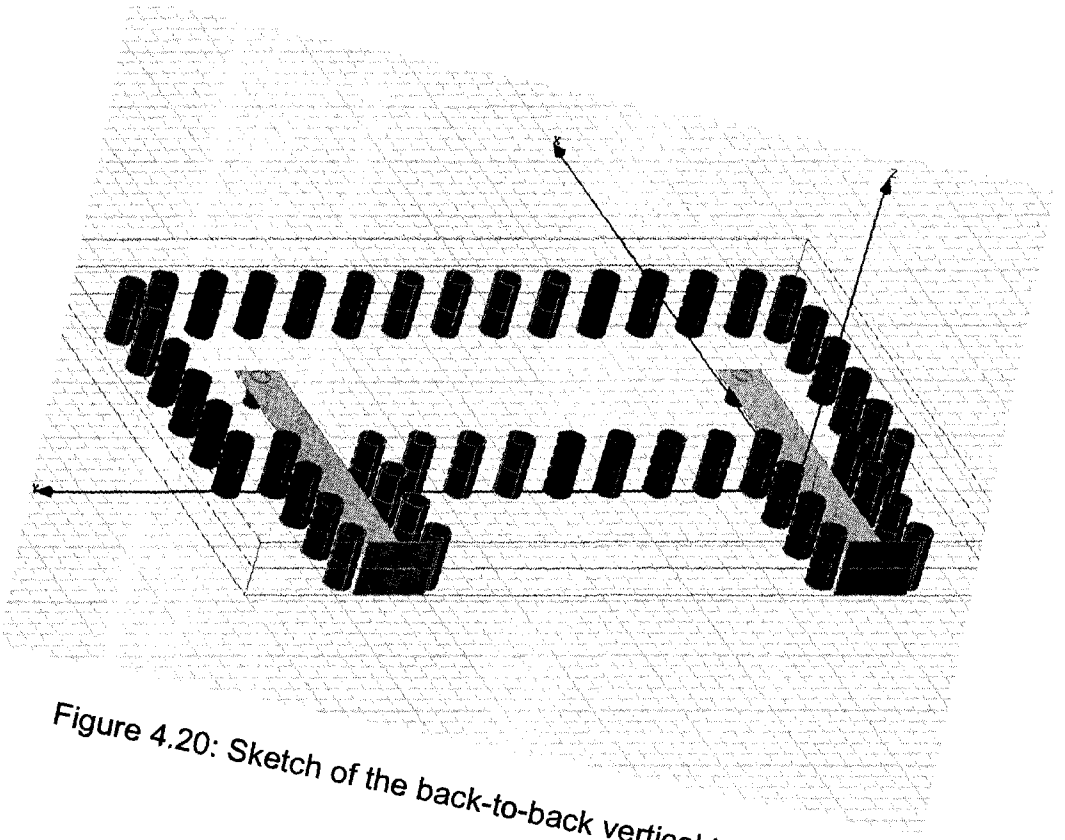

Figure 4.20: Sketch of the back-to-back vertical transition.

The wave ports in the simulation are placed at the beginning of the two shielded striplines. Each wave port has a characteristic impedance of 50Ω. The three back-to-back transitions for the C band, Ku band and Ka band are given in figures 4.21, 4.18 & 4.22 respectively. In all three transitions the bandwidth for a return loss less than -20dB was measured to be at least 20% and ranged up to 35%.

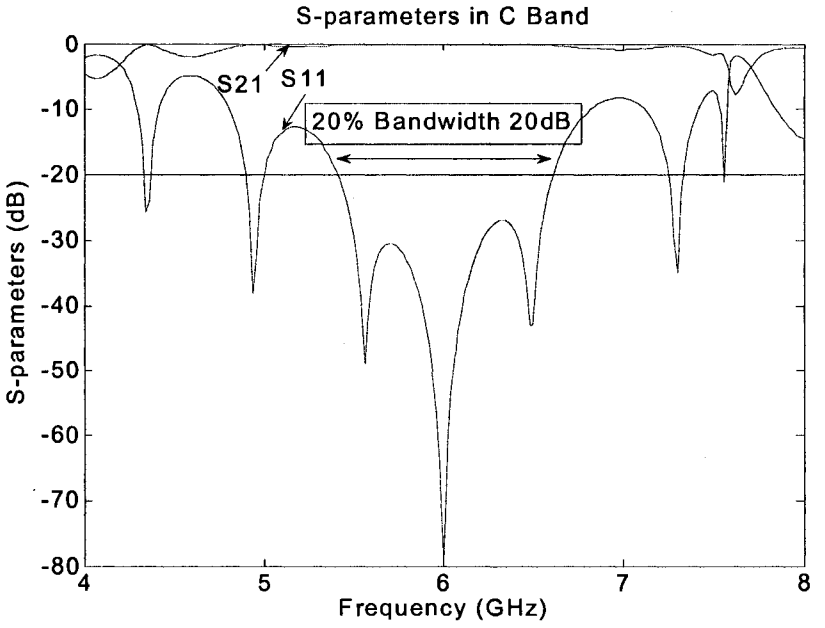

Figure 4.21: Back-to-back transition for the C band.

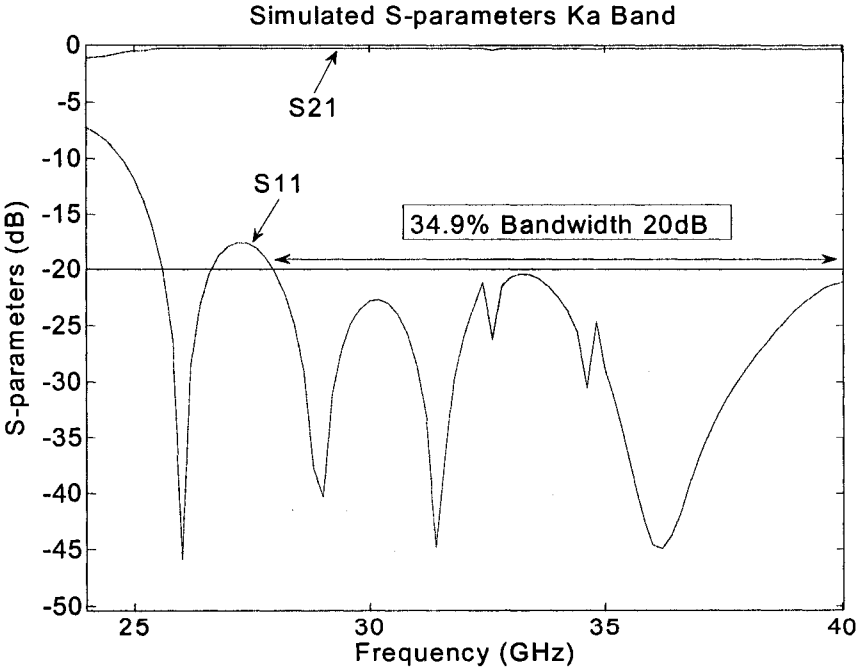

Figure 4.22: Back-to-back transition for the Ka band.

A back-to-back transition was fabricated for the C-band. A photo of the back-to-back transition can be found in figure 4.23.

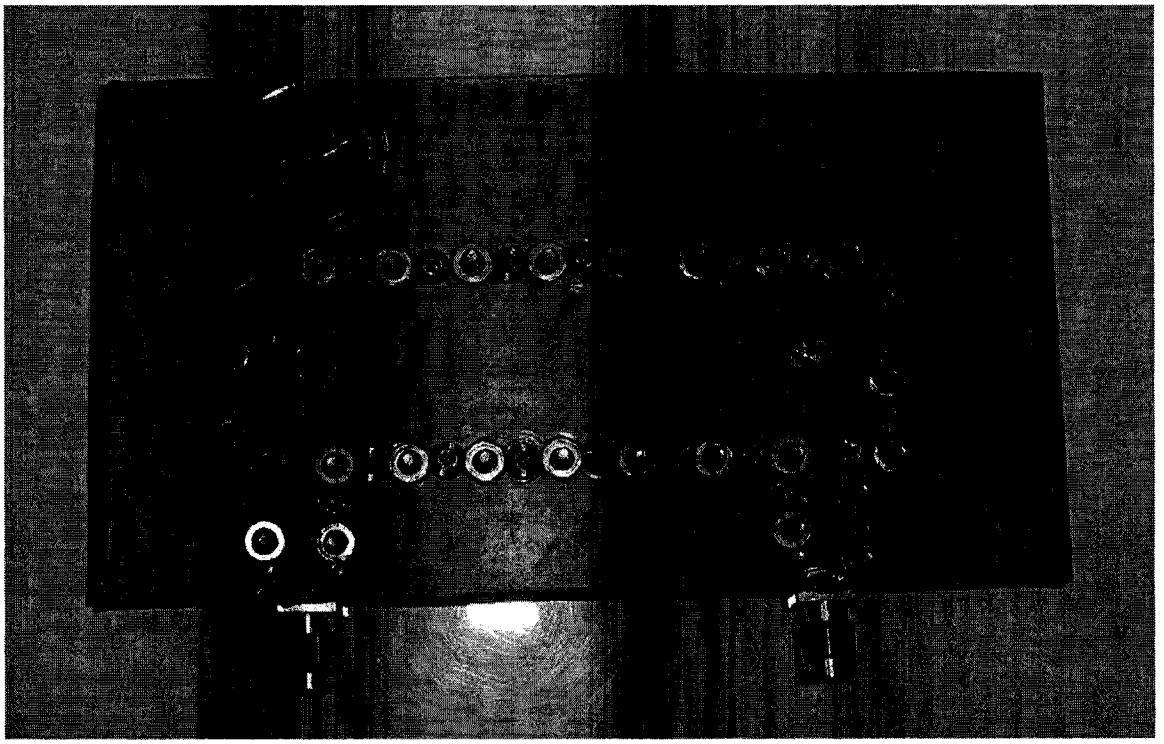

Figure 4.23: Photograph of back-to-back vertical transition.

The measured results of the back-to-back vertical transition are displayed in figure 4.24.

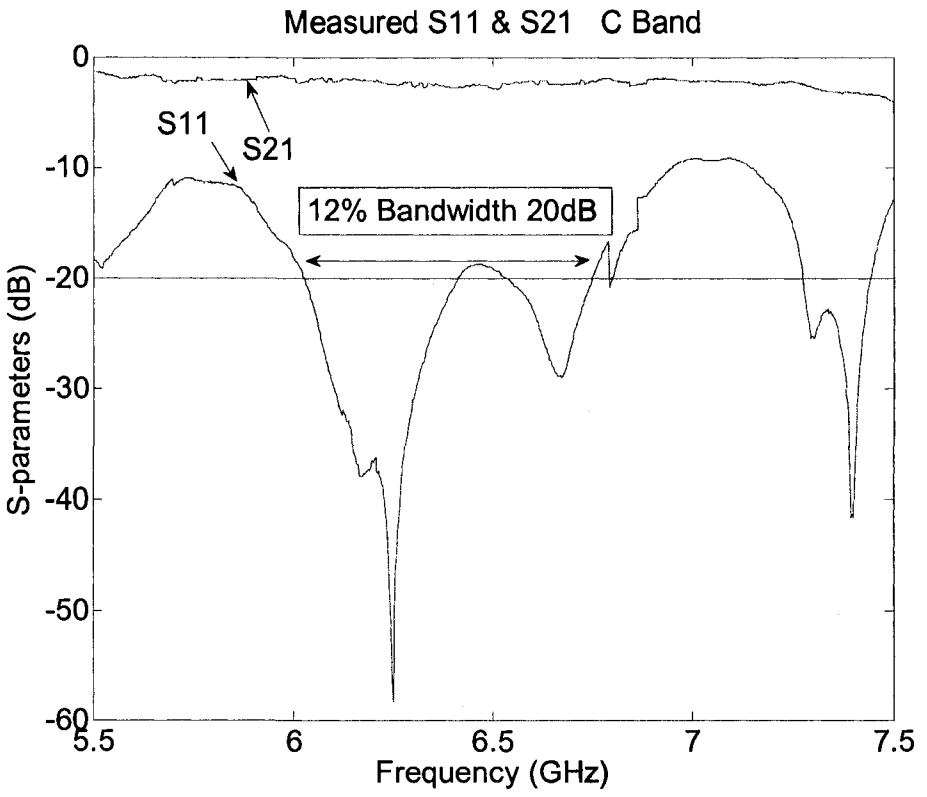

Figure 4.24: Measured results of back-to-back vertical transition.

When comparing the measured results to the simulated results one notices that the two curves are not in agreement. The measured results has a shorter bandwidth just a 12% bandwidth at 20dB instead of 20% and the passband is shifted a couple hundred megahertz to the higher frequencies. The reason for the dissimilarities is that the transition was not professionally fabricated. It was fabricated by hand. The copper sheet on one side of each substrate was sandpapered down so that the two substrates could be sandwiched together. This caused some slight unevenness along the middle of the circuit where the two substrates meet. It also slightly diminished the height of the circuit as well. The stripline was fabricated by cutting out a thin piece of electrical tape and sticking it onto the substrate. The small size of the trace makes it difficult to accurately cut out the

inner conductor of the stripline. The via holes were implemented by drilling holes into the substrate and attaching screws through the holes. The imperfections mentioned above caused the geometry of the circuit to change slightly. Since we are dealing with microwave frequencies the wavelength is very small and thus these slight changes in the geometry can have a rather stark affect on the expected outcome. Although the measured and simulated results are not in good agreement, the measured results show that the transition does in fact work and if the transition is professionally fabricated such that the geometry of the circuit is accurately maintained the measured results can only improve.

4.6 Transformation of Dielectric-Filled Waveguide to Substrate Integrated Waveguide

The transformation of a dielectric-filled waveguide into a SIW requires replacing the metallic sidewalls of the waveguide by two rows of metallic via holes. The SIW must have the same guided wave characteristics as the dielectric-filled waveguide. As to designing the SIW the size and placement of the via holes is crucial. The three parameters of the via holes is the diameter d, the spacing between adjacent vias s and the distance between the two rows of via holes a. The theory on substrate integrated waveguides is given in section 3.6. Following equation (3.35) the ratio between the spacing and the diameter will be equal to $s/d=2$. The circuit will be composed of two substrates stacked upon each other with each having a thickness of 30mil. Due to fabrication limitations the diameter of the via hole can be no smaller than the thickness of the substrate. Since the substrate thickness of the circuit is 2X30mils and following the guidance of equation (3.36) the diameter of the via holes is chosen to be 60mil. The s/d ratio was chosen to be

2 so the spacing between adjacent via holes will be 120mil. Choosing $d=60mil$ and $s=120mil$ will ensure that the leakage loss between the posts will be minimal and will have a negligible impact on the performance of the SIW.

The size and spacing of the metallic posts have been determined, and now the distance between the two rows of via holes, a, must be calculated. This parameter serves the same function as the width of a rectangular waveguide a_{RWG}. The value of a determines the cut-off frequencies of the different modes that can exist in the SIW [1,3,11,13]. The goal is to choose a such that the SIW exhibit's the same guided-wave characteristics as a regular rectangular waveguide with a width of $a_{RWG}=9mm$. The propagation constant of a rectangular waveguide with a width $a_{RWG}=9mm$ is $\beta=410.76$. The SIW must be designed to have the same propagation constant. An initial estimate of the parameter a can be found with equation (3.44). A more accurate method involving the calculation of the propagation constant of the SIW described in section 3.6 will be used. Following this method two identical substrate integrated waveguides of different lengths are simulated using HFSS and their propagation constant extracted.

SIW Physical Characteristics	**Numerical Value**
Dielectric Constant, ε_r	2.94
Via Hole Diameter, d	60mil
Via Hole Spacing, s	120mil
Width, a	390mil
RWG Equivalent Width, a_{RWG}	9mm
Thickness, b	60mil

Table 4.3: Dimensions of Substrate Integrated Waveguide.

Two SIW sections of lengths $L_1=940mil$ & $L_2=700mil$ excited by a TE_{10} mode wave were simulated with a wave port at each end. The SIW characteristics are given in table 4.3. The phase difference between the two ports was measured to be $\Delta\phi=1.83rad$ and used to determine the propagation constant of the SIW with equation (3.45). The propagation constant was calculated to be $\beta_{SIW}=411.46$. This is very close to the propagation constant of a waveguide with $a_{RWG}=9mm$. To further study the ability of the SIW to mimic the dielectric-filled waveguide, a transmission line consisting of a section of the SIW inserted in between two dielectric-filled waveguide sections was simulated. The S-parameters, displayed in figure 4.25 & 4.26, indicate how well the SIW is matched to the desired equivalent waveguide at the operating frequency of 15GHz and over the whole K_u frequency band.

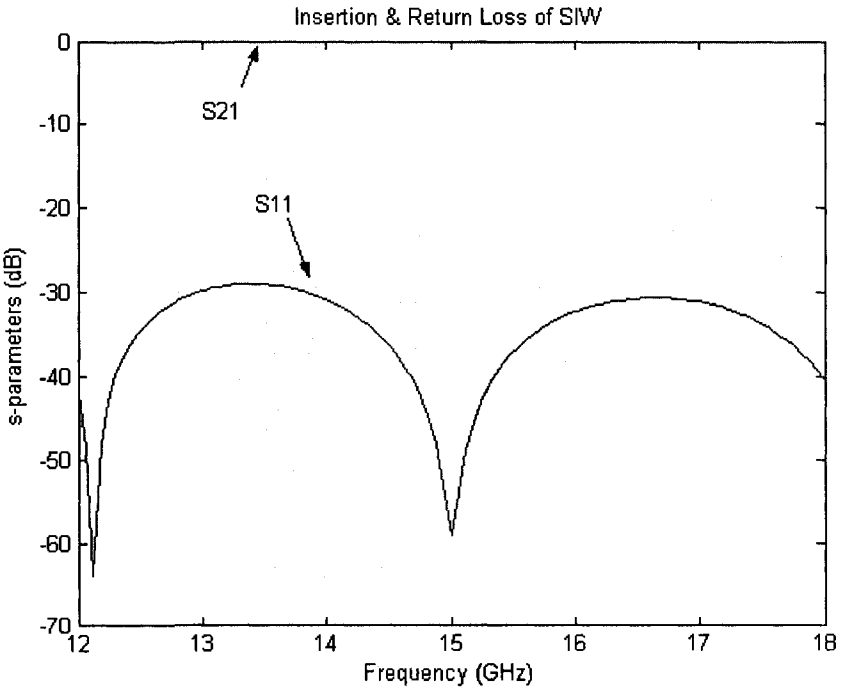

Figure 4.25: Insertion & Return Loss of a SIW sandwiched in between two waveguide sections.

A closer look at the insertion loss of the SIW can be seen by reviewing figure 4.26. The insertion loss is less than 0.2dB. This indicates that the via holes are properly located so that the electromagnetic fields are contained within the SIW.

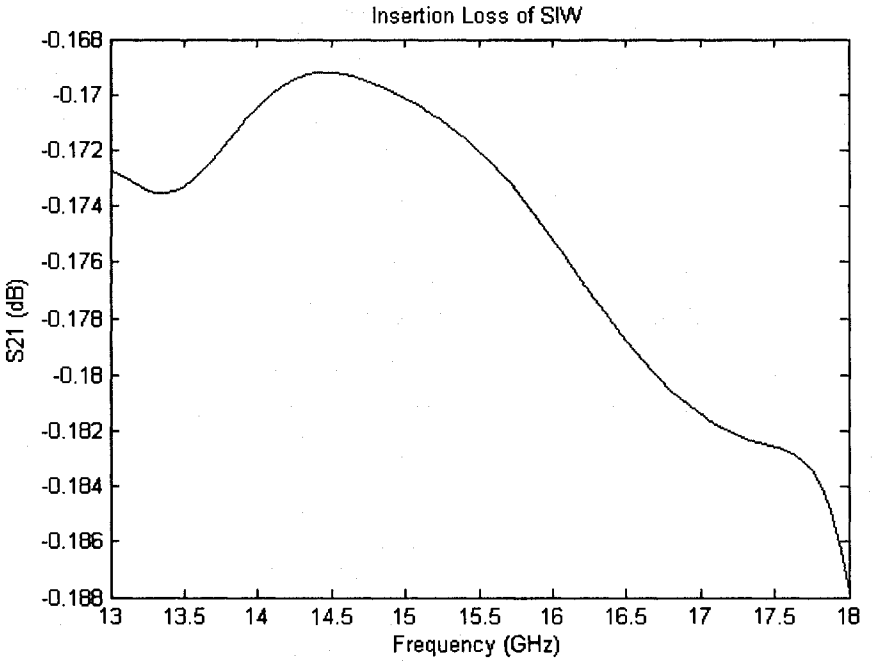

Figure 4.26: Insertion Loss of SIW sandwiched in between two waveguides.

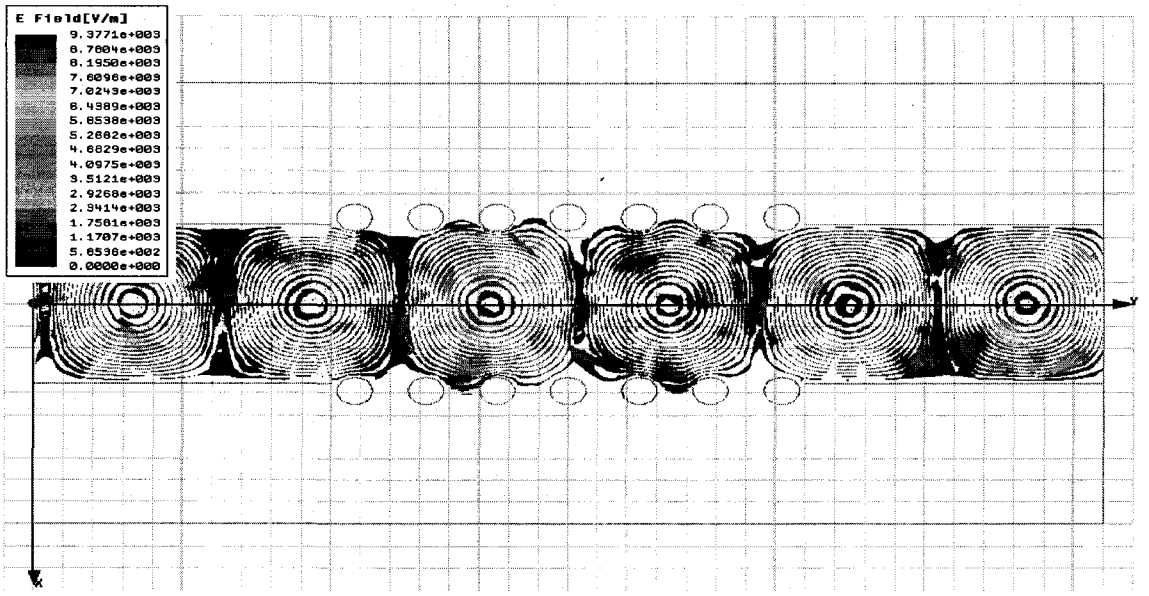

Figure 4.27: Plot of the electric fields propagating through the dielectric-filled waveguide and SIW sections.

Figure 4.27 shows that the fields are well contained within the two rows of via holes.

4.7 Transformation of a Rectangular Coax into a Shielded Stripline

In section 4.4 the dimensions of a rectangular coax were calculated to give a characteristic impedance of 50Ω. The vertical sidewalls of the structure are difficult to construct in a substrate without physically disrupting the substrate itself. Just as in the case of the waveguide, the sidewalls are replaced with a row of cylindrical metallic posts. The dimensions and relative placement of the via holes are governed by the same parameters as in the SIW case. The size of the via holes must keep the electromagnetic fields within the structure and shield them from other unwanted fields that could be within the proximity of the stripline [1,3]. Following the same guidelines discussed in section 3.6 & 3.7 the dimensions of the post are the same as the ones used to construct the

SIW. The only difference is the distance separating the two rows of post. This distance must be chosen such that the characteristic impedance of the shielded stripline is 50Ω. The performance of the shielded stripline can be simulated with HFSS by a placing a section of the shielded stripline in between two sections of the rectangular coax. The separation distance *a* of the shielded stripline's posts were optimized in order to get the best possible match to a 50Ω rectangular coax line. Table 4.4 displays the dimensions of the shielded stripline. The insertion loss and return loss of the shielded stripline are plotted in figure 4.28.

Shielded Stripline Dimensions	**Numerical Value**
Dielectric Constant, ε_r	2.94
Inner Conductor Width, w_i	40mil
Inner Conductor Thickness, t	0mil
Outer Conductor Height, h	60mil
Via Hole Diameter, *d*	60mil
Via Hole Spacing, *s*	120mil
Outer Conductor Width, *a*	185mil
Equivalent Outer Conductor Width, a_{RC}	155mil

Table 4.4: Dimensions of the shielded stripline.

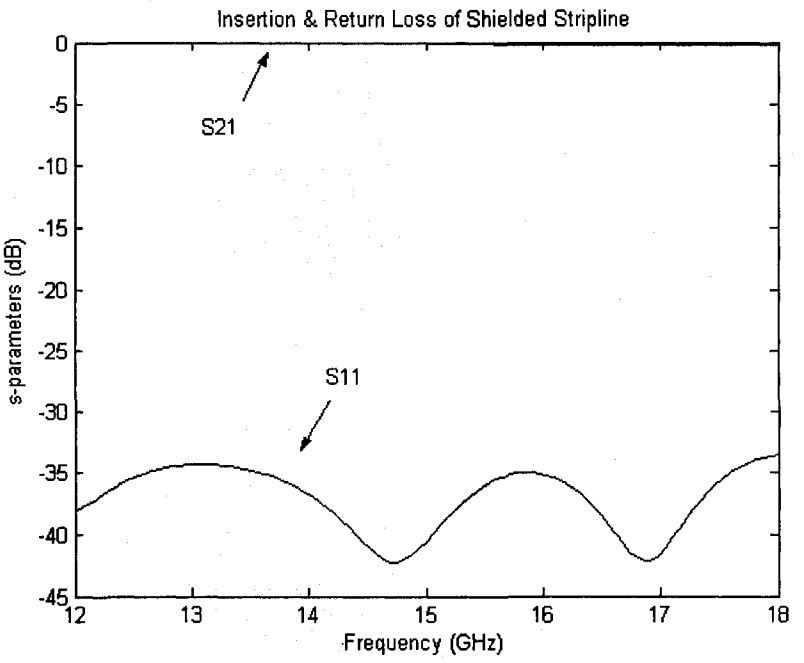

Figure 4.28: Insertion loss & return loss of shielded stripline sandwiched in between two rectangular coax sections.

Figure 4.28 demonstrates that the shielded stripline is well matched to the 50Ω rectangular coax line. Due to the geometry of the stripline it can support a TEM mode wave which has the characteristic of a large bandwidth.

4.8 Slotted Substrate Integrated Waveguide Antenna Fed by a Shielded Stripline

The theory, design and simulation of a slotted waveguide antenna, shielded stripline, vertical transition between a stripline and waveguide and the method that integrates these circuits in a substrate with use of well placed metallic via holes have been presented in previous sections of this thesis. In this section all these individual circuits will be simulated together in one double-stacked substrate. The performance of the circuit will be assessed according to how well the input signal propagates through the circuit and

radiates out the 8 slots and on its radiation pattern characteristics. A slotted SIW antenna with 8 longitudinal slots of uniform amplitude fed by a shielded stripline is simulated with HFSS. A vertical transition is used to link the shielded stripline to the SIW. A diagram of the circuit is shown in figure 4.29.

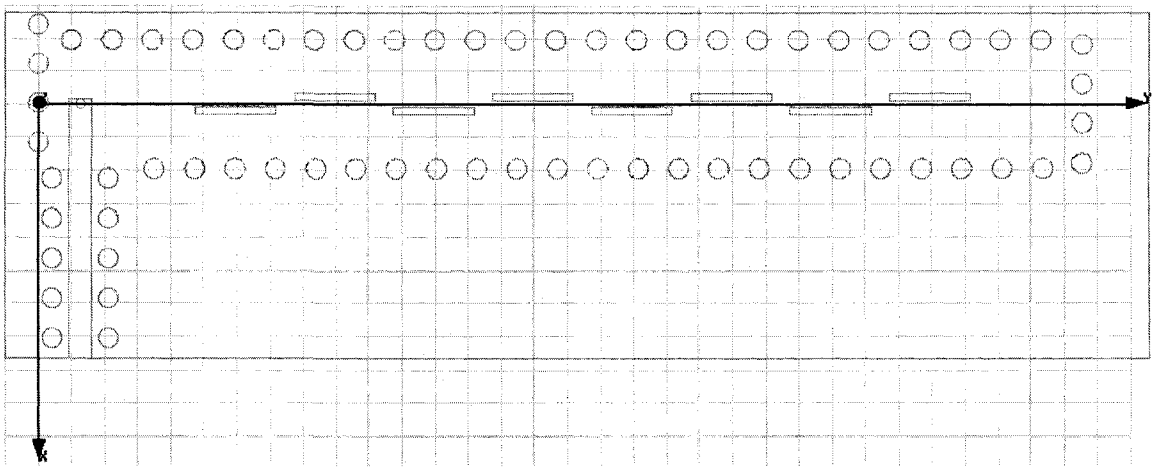

Figure 4.29: Top view of slotted SIW antenna fed by a shielded stripline.

The radiation pattern of the antenna is plotted in figure 4.30 & 4.31. The radiation pattern shows that the antenna has a half-power beamwidth of 17°. The two main sidelobes are evenly distributed 14dB below the main beam. The E-plane is almost identical to the E-plane radiation pattern of the perfectly fed slotted waveguide. However quite a noticeable difference is observed in the H-plane. Instead of one smooth curve as shown in figure 4.13, which is the expected pattern of a single slot, the H-plane has a dip in the broadside direction. This causes the H-plane pattern to have two main peaks located at ±33°. The vertical transition appears to affect the H-plane radiation pattern of the antenna.

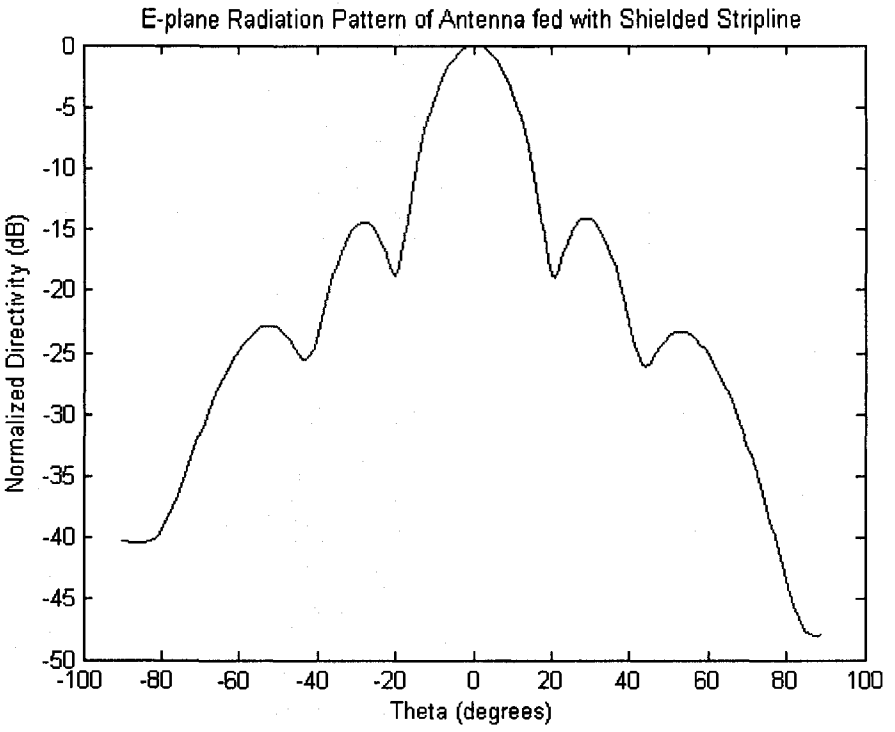

Figure 4.30: Radiation pattern of the antenna shown in figure 4.29.

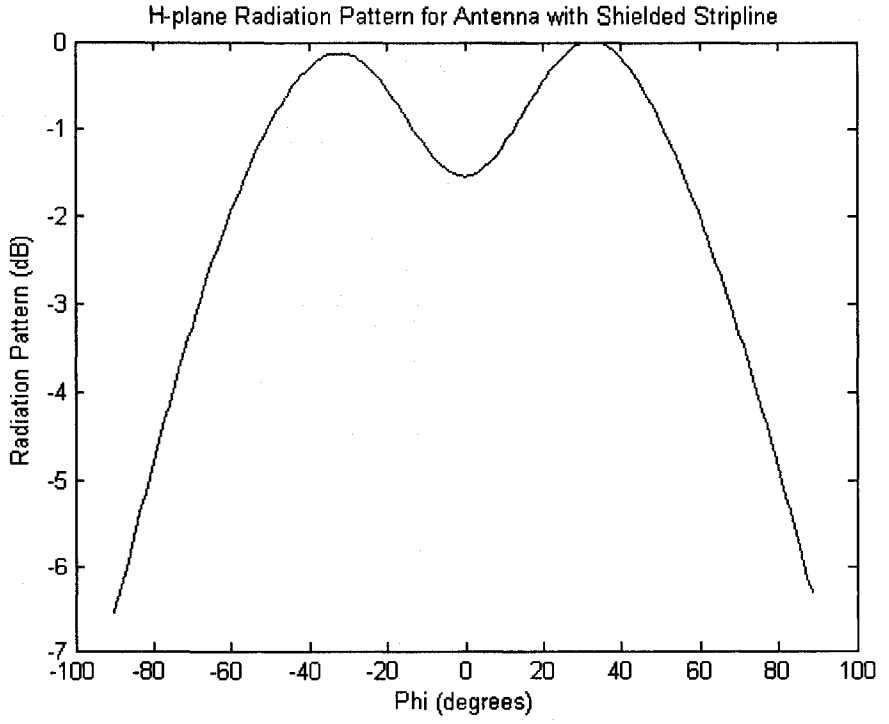

Figure 4.31: H-plane Radiation Pattern of antenna shown in figure 4.29.

The return loss, plotted in figure 4.32, indicates how efficiently the circuit is able to radiate the input signal. It also shows the bandwidth of the antenna which is measured to be just over 1GHz, this is equivalent to a 7% bandwidth.

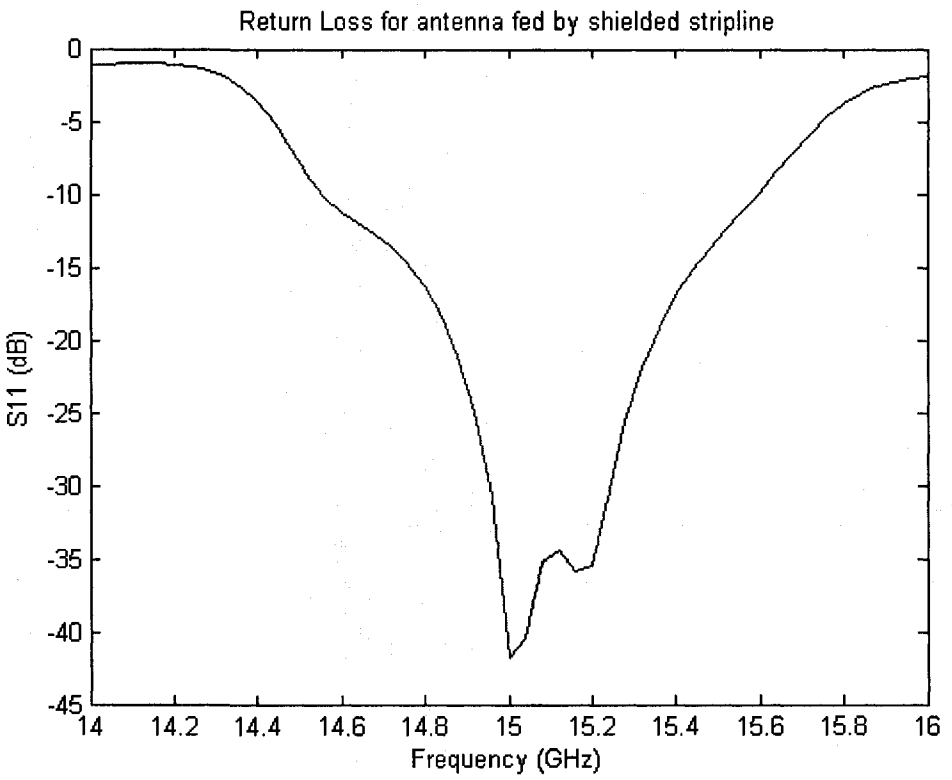

Figure 4.32: Return loss for the antenna shown in figure 4.29.

The circuit described above is designed to be fed by a 50Ω source at the shielded stripline. Due to the fabrication procedure of the via holes soldering a microwave connector to the shielded stripline is not feasible. The proposed solution to this problem is to connect a microstrip line to the shielded stripline. Since the microstrip line does not have a second substrate covering its trace, an SMA connector can be easily soldered onto the microstrip's conductor. This additional transmission line added to the circuit will

require a transition that connects the 50Ω microstrip line to the 50Ω shielded stripline. The return loss of the circuit will degrade slightly due to the additional transition, but it is a necessary part of the circuit if one wants to experimentally test the performance of the circuit. The microstrip line is connected to the shielded stripline through a simple tapered transition. A sketch of the entire circuit including the microstrip line, shielded stripline and slotted SIW antenna can be found in figure 4.33.

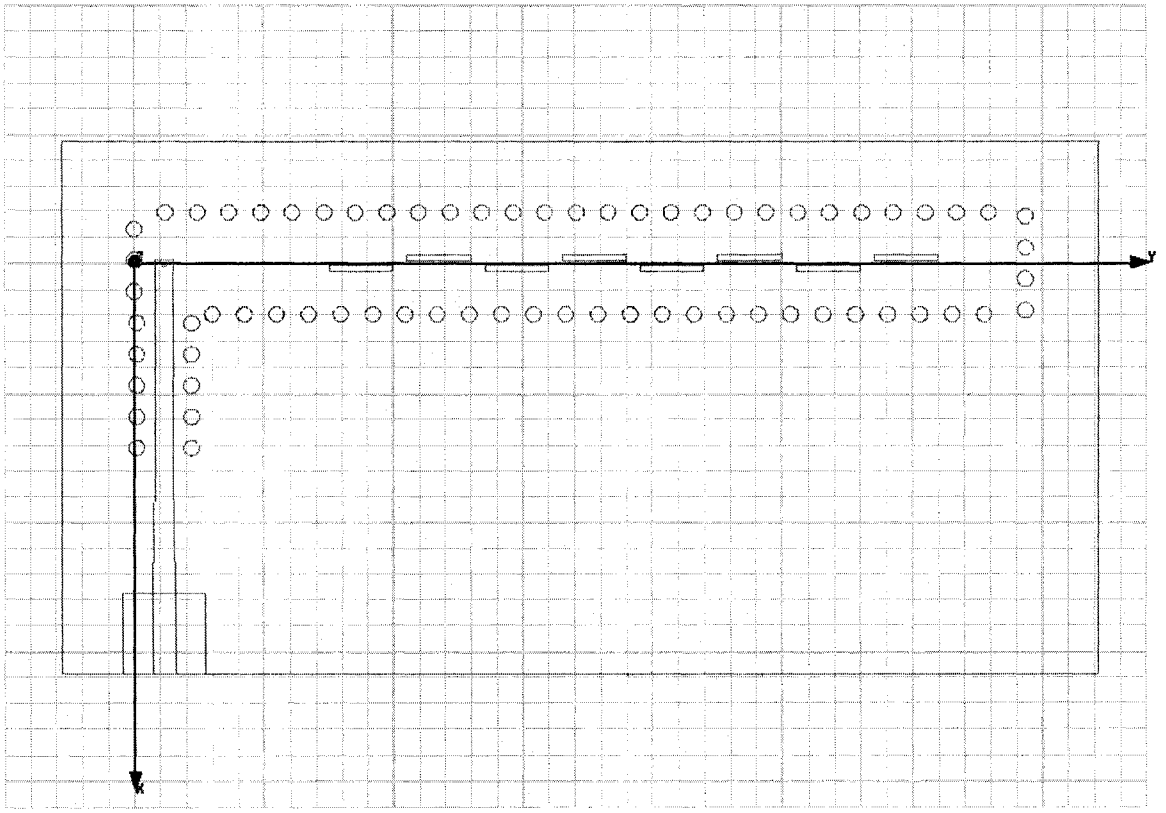

Figure 4.33: Sketch of the antenna fed by a shielded stripline preceded by a microstrip line.

The E-plane radiation pattern can be found in figure 4.34. The sidelobes are 13.5dB below the main beam. The directivity and gain of the antenna have not changed. There is however some backlobe radiation due to the microstrip.

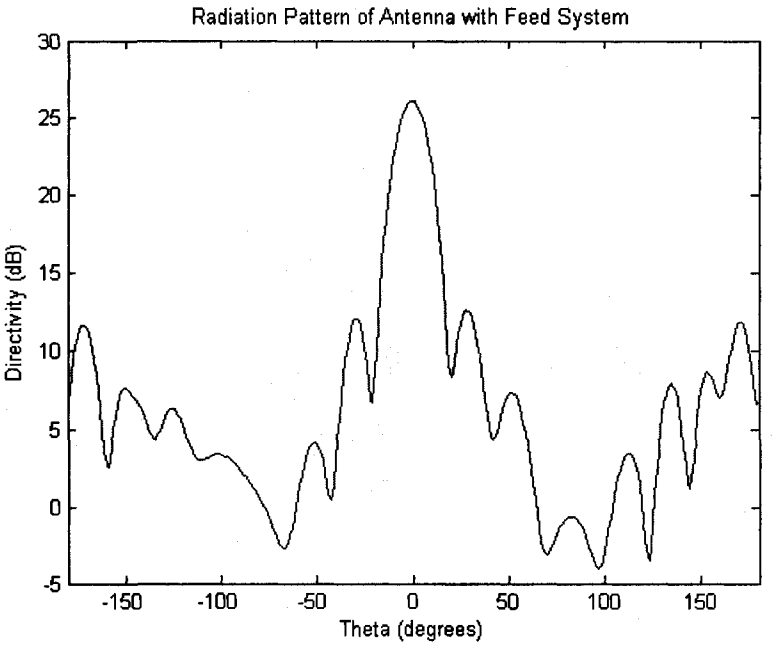

Figure 4.34: E-plane radiation pattern of the antenna shown in figure 4.33.

The return loss of the antenna is plotted in figure 4.35. A 10% bandwidth is achieved for a return loss of less than -10dB.

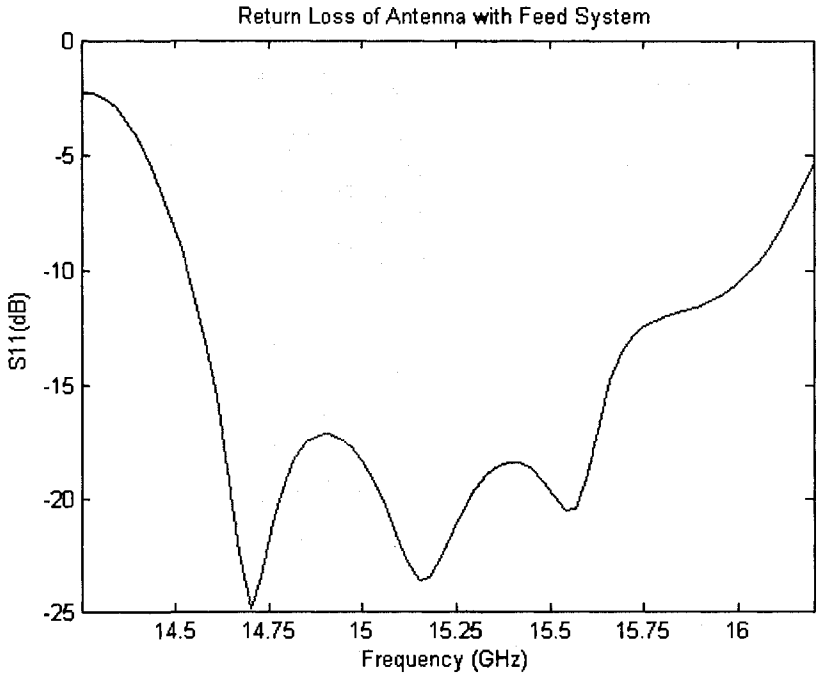

Figure 4.35: Return loss of the antenna fed by both the stripline and microstrip.

Chapter 5

Conclusion and Future Work

5.1 Conclusion

The ability to reliably mass manufacture microwave circuits is a very important topic. The cost of a circuit significantly increases if the circuit cannot be manufactured in large numbers quickly and reliably. The bulky size of waveguides and the conventional transitions used to connect the waveguides to other planar circuits makes the mass manufacturing of circuits that include waveguides very difficult and costly. However the waveguide is a very useful transmission line and has many applications. One such application is the slotted waveguide antenna, a durable and robust antenna that can provide a large gain. Substrate integrate waveguides allow an equivalent rectangular waveguide to be realized inside the substrate. The SIW can be designed to have the same propagation constant, characteristic impedance and cut-off frequencies as a rectangular waveguide [1,3,11]. The SIW not only eliminates the need for expensive transitions between planar circuits and waveguides, but it also gives manufacturers the ability to reliably mass produce microwave circuits that incorporate waveguides. In this thesis the SIW technology is used to design a slotted SIW antenna that is fed by a shielded stripline. A vertical transition that connects the shielded stripline to the SIW though a metallic via hole that acts as a current probe is proposed. The transition is based upon previous work [17, 32-35] on a transition between a coaxial cable and a waveguide through the use of a probe. The transition was studied and simulated over three different frequency bands. Good insertion loss and return loss characteristics of the transition were observed. The back-to-back transitions showed a bandwidth that ranged between 20-35% for return loss

better than 20dB depending of the frequency band. A back-to-back transition was fabricated in the C-band and the measured results show that the vertical transition does indeed function. Simulations have shown that the s-parameter characteristics depend considerably on the radius of the current probe that connects the inner conductor of the shielded stripline to the SIW. Previous works [4,30,48] have used a tapered microstrip line to feed substrate integrated waveguides. The proposed vertical transition offers an alternative method to feed an SIW and the results show that the transition has generally a larger bandwidth over the tapered microstrip transition. This transition allows the designer to feed a slotted SIW antenna in a multi-layered environment where the conductor carrying the signal might not be on the top plane of the circuit.

A slotted SIW antenna of 8 longitudinal slots of uniform amplitude was designed and simulated. The antenna including the feeding scheme showed a good radiation pattern with even sidelobes measured 14dB below the main beam. The addition of the vertical transition caused the H-plane radiation pattern of the antenna to change, however the E-plane pattern remained the same. The simulated antenna including the feed network shows a 10% impedance bandwidth about the 15GHz operating frequency.

An additional transition was designed to link a microstrip line to a shielded stripline. A tapered transition was employed to connect the two transmission lines. This transition is necessary for the physical fabrication and experimental measuring of the circuit. The microstrip line allows a SMA connector to be attached to the circuit so that measurements can be performed and antenna's performance can be judged.

5.2 Future Work

Substrate integrated waveguides are a relatively new type of microwave transmission line and there is a fair amount of areas left to study. A two dimensional planar array of slotted SIW with beam steering capabilities can be studied. The feeding mechanism presented in this thesis could possibly be modified to feed an array of slotted substrate integrated waveguides. Another potential future research area can be a traveling-wave fed slotted SIW antenna. This type of antenna can be studied to develop larger impedance bandwidths.

References

[1] D. Deslandes, K. Wu, "Accurate modeling, wave mechanisms, and design considerations of a substrate integrated waveguide," *IEEE Trans. Microw. Theory Tech.*, vol. 54, no.6, June 2006.

[2] Website, http://www.digdice.com/wp-content/uploads/2007/10/swg1.jpg.

[3] F. Xu and K. Wu, "Guided-wave and leakage characteristics of substrate integrated waveguide" *IEEE Trans. Microw. Theory Tech.*, vol. 53, no. 1, pp. 66-73, Jan. 2005.

[4] D.Deslandes and K. Wu, "Integrated microstrip and rectangular waveguide in planar form" *IEEE Microw. Wireless Compon. Lett.*, vol. 11, no.2, pp. 68-70, Feb. 2001.

[5] D. Deslandes and K. Wu, "Analysis and design of current probe transition form grounded coplanar waveguide to substrate integrated rectangular waveguides", *IEEE Trans. Microw. Theory Tech.*, vol. 53, no. 8, Aug. 2005.

[6] M. T. Rashid, A. R. Sebak, "Design and modeling of a linear array of longitudinal slot on substrate integrated waveguide", *NRSC,* Mar. 2007.

[7] R.S. Elliot, "Antenna Theory & Design", *Wiley-IEEE Press; Revised Edition,* 1976.

[8] R.S. Elliot, "An improved design procedure for small arrays of shunt slots" *IEEE Trans. Antennas Propagat.*, vol. AP-31, pp. 48-53, Jan. 1983

[9] R.S. Elliot and W.R. O'Loughlin, "The design of slot arrays including internal mutual coupling," *IEEE Trans. Antennas Propagat.*, vol. AP-34, pp. 1149-1154, Sept. 1986.

[10] Ecoly Polytechnique, "PCB Guidelines"

[11] Y. Cassivi, L.Perreprini, P. Arcioni, M. Bressan, K. Wu, and G. Conciauro, "Dispersion characteristics of subsrtate integrated rectangular waveguide", *IEEE Microw. Wireless Compon. Lett.*, vol. 12, no. 9, pp. 333-335, Sept. 2002.

[12] D. M. Pozar, *Microwave Engineering,* 3rd ed. New York: Wiley, 2005.

[13] L. Yan, W. Hong, K. Wu, and T.J. Cui, "Investigations on the propagation characteristics of the substrate integrated waveguide based on the method of lines" *Proc. Inst. Elect. Eng.-Microw. Antennas Propag.,* vol.152, pp. 35-42, Feb. 2005.

[14] Z. Weng, R. Guo, and Y.C. Jiao, "Design and experiment on substrate integrated waveguide resonant slot array antenna at Ku-band", *ISAPE Antennas Propagat EM Theory.,* Oct. 2006.

[15] H. Nam, T-S Yun, K-B Kim, K-C Yoon, and J-C Lee, "Ku-band transition between microstrip and substrate integrated waveguide (SIW)," *Asia-Pacific Conf. Proc.,* vol. 1, Dec. 2005.

[16] Y. Ding, and K. Wu, "Substrate integrated waveguide-to-microstrip transition in multi-layer substrate," *IEEE Trans. Microw. Theory & Tech.,* vol. 55, no. 12, pp.2839-2844, Dec. 2007.

[17] R.F. Harrington, "Time-harmonic electromagnetic fields", Wiley-IEEE Press; 1st edition.

[18] L. Josefsson, "Slot coupling and scattering," *Anten. & Propag. SIS,* vol. 2 pp. 942-945, May 1990.

[19] L. Josefsson, "Analysis of longitudinal slots in rectangular waveguides," *IEEE Trans. Antenn. & Porpag.,* vol. 35, no. 12, pp. 1351-1357, Dec. 1987.

[20] M-Q Qi, W. Wang, and M-p Jin, "A method of calculating admittance of waveguide slot," *Microw. Conf. Proc. APMC,* vol. 4 pp.3, Dec. 2005.

[21] S.R. Rengarajan, M. Steinbeck, "Longitudinal slots in dielectric filled rectangular waveguides," *Anten. & Propag. SIS,* vol. 2, pp. 1276-1279, Jun. 1991.

[22] M. Himdi, and S. Chainon, "Transmission line model for longitudinal slot dielectric-filled waveguide," *IEEE Anten. & Propag. SIS,* vol. 4, pp. 424-427, Jun. 2002.

[23] S. Martynuk, "Investigation and optimization of a waveguide slot antenna array by finite-difference time-domain method," *International Conf. MMET,* vol. 1, pp. 166-168, Sept. 2000.

[24] C-G Jan, R-B Wu, P. Ilsu, and D-C Chang, "Analysis of edge slots in rectangular waveguide with finite waveguide wall thickness," *IEEE Trans. Anten. & Propag.,* vol. 44, pp. 1120-1126, Aug. 1996.

[25] C. A. Balanis, "Antenna Theory: Analysis & Design", Wiley-Interscience; 3rd edition, 2005.

[26] M.J. Erlich, and J. Short, "Mutual coupling considerations in linear-slot array design," *Proc. of the IRE,* vol. 42 no. 6, pp. 956-961, Jun. 1954.

[27] A. Morini, T. Rozzi, and G. Venanzoni, "On the analysis of slotted waveguide arrays," *IEEE Trans. Anten. & Propag.,* vol. 54, no. 7, pp. 2016-2021, Jul. 2006.

[28] S.R. Rengarajan, "Higher order mode coupling effects in the feeding waveguide of a planar slot array," *IEEE Trans. Microw. Theory & Tech.,* vol. 39, pp. 1219-1223, Jul. 1991.

[29] W. Wang, J. Jin, J-G Lu, and S-S Zhong, "Waveguide slotted antenna array with broadband, dual-polarization and low cross-polarization for X-band SAR applications," *IEEE International Radar Conference,* pp. 653-656, May 2005.

[30] L. Yan, W. Hong, G. Hua, J. Chen, K. Wu and T.J. Cui, "Simulation and experiment on SIW slot array antennas", *IEEE Microw. Wireless Compon. Lett.*, vol. 14, no. 9, Sept. 2004.

[31] T-S Chen, "Determination of the capacitance, inductance, and characteristic impedance of rectangular lines," *IEEE Trans. Microw. Theory Tech.,* vol. 8, issue 5, pp. 510-519, Sept. 1960.

[32] M. Wong, B. MacIntosh-Hobson, A. Sebak, "A New Feed Method for the Substrate Integrated Waveguide Using the Substrate Integrate Rectangular Coaxial line," *Antem Conference 2007.*

[33] M.E. Bialkowski, P.J. Khan, "Determination of the admittance of a general waveguide-coaxial line junction," *IEEE Trans.,* vol. 4, pp. 465-467, 1984.

[34] R.B. Keam, A.G. Williamson, "Analysis of a coaxial-line/rectangular waveguide junction with a dielectrically sheathed probe," *Electron. Lett.,* vol. 28, pp. 240-241, 1992.

[35] R.B. Keam, A.G. Williamson, "Analysis and design of a coaxial-line/rectangular waveguide junction with a dielectrically sheathed centre probe," *Proc. Asia-Pacific Microw. Conf.,* pp.845-848, Adelaide, Australia, 1992.

[36] A.G. Williamson, "Analysis and modeling of a coaxial-line/rectangular-waveguide junction," *IEE Proc. H,* vol. 129, pp.262-270, 1982.

[37] R.B. Keam, A.G. Williamson, "Coaxially driven dielectrically sheathed post in a rectangular waveguide," *Microw. Opt. Tech. Lett.,* pp. 230-234, 1993.

[38] R.B. Keam, A.G. Williamson, "Broadband design of coaxial line/rectangular waveguide probe transition," *IEE Proc. Microw. Antenn. & Propag.,* vol. 141, pp. 53-58, Feb. 1994.

[39] J.M. Jarem, "A multifilament method-of-moments solution for the input impedance of a probe-excited semi-infinite waveguide," *IEEE Trans. Microwave Theory & Tech.,* vol. 35, no. 1, pp. 14-19, Jan. 1987.

[40] H. Yao and K.A. Zaki, "Modeling of generalized coaxial probes in rectangular waveguides," *IEEE Trans. Microw. Theory & Tech.,* vol. 43, no. 12, pp. 2805-2811, Dec. 1995.

[41] M. E. Bialkowski, "Analysis of a coaxial-to-waveguide adaptor including a disc-ended probe and a tuning post," *IEEE Trans. Microw. Theory & Tech.,* vol. 43, no. 2, pp. 344-349, Feb. 1995.

[42] J. Liang, H. Chang and K.A. Zaki, "Coaxial probe modeling in waveguides and cavities," *IEEE Trans. Microw. Theory & Tech.,* vol. 40, no. 12, pp. 2172-2180, Dec. 1992.

[43] J.A. Ruiz-Cruz, K.A. Zaki, J.M. Rebollar, "Mode-matching analysis of a coaxial-to-stripline discontinuity applied to the modeling of a coaxial probe," *IEEE Ant. & Prop. International Syposium,* vol. 2, pp. 2139-2142, Jun. 2004.

[44] A.M. Helaly, J.M. Jarem, "Input impedance of a probe excited semi-infinite rectangular waveguide with a tuning post," *Southeastern Syposium on System Theory,* pp. 161-167, Mar. 1990.

[45] D. Deslandes and K. Wu, "Design consideration and performance analysis of substrate integrated waveguide components" *Proc. 32th Eur. Microw. Conf.,* Milan, Italy, Sept. 2002, vol. 2, pp. 881-884.

[46] F. Xu and K. Wu, "Numerical multimode calibration technique for extraction of complex propagation constants of substrate integrated waveguide" *IEEE MTT-S Int. Microw. Symp. Dig.,* pp. 1229-1232, Jun. 2004.

[47] F. Xu, Y. Zhang, W. Hong, K. Wu, and T.J. Cui, "Finite-difference frequency-domain algorithm for modeling guided-wave properties of substrate integrated

waveguide" *IEEE Trans. Microw. Theory Tech.,* vol. 51, no. 11, pp. 2221-2227, Nov. 2003.

[48] L. Yan, W. Hong, and K. Wu, "Simulation and experiment on substrate integrated monopulse antenna", *IEEE Antennas Propagat.,* vol. 1A, pp. 528-531, Jul. 2005.

[49] A.F. Stevenson, "Theory of slots in rectangular waveguides," *J. Appl. Phys.,* vol. 19, pp. 24-38, January 1948.

[50] T. Vu Khac, C. Carson, "Impedance properties of a longitudinal slot antenna in the broad face of a rectangular waveguide," *Antenn. & Propag. IEEE Trans.,* vol. 21, no.5, pp. 708-710, Sept. 1973.

[51] G. Hua, W. Hong, X. H. Sun, H. X. Zhou, "Design of an omnidirectional line array with SIW longitudinal slot antenna," *ICMMT,* vol. 3, pp. 1114-1117, April 2008.

[52] Z. Zeng, W. Hong, Z. Kuai, H. Tang, J. Chen, "The design and experiment of a dual-band omni-directional SIW slot array antenna," *APMC,* Dec. 2007.

[53] H-C Lu, T-H Chu, "Equivalent circuit of radiating longitudinal slots in substrate integrated waveguide," *IEEE Antennas Propag.,* vol. 3, pp. 2341-2344, Jun. 2004.

[54] S. Germain, D. Deslandes, K. Wu, "Development of substrate integrated waveguide power dividers," *IEEE CCECE,* vol. 3 pp. 1921-1924, May 2003.

[55] C-H Tseng, T-H Chu, "Measurement of frequency-dependent equivalent width of substrate integrated waveguide," *IEEE Trans. Microw. Theory Tech.,* vol. 54, no. 4, April 2006.

[56] Z-P Cong, P. Wang, P-H Li, "Analysis and experiment of transition between micro-strip and a miniaturization substrate integrated waveguide (SIW)," *ISAPE,* Oct. 2006.

[57] W. Hong, "Development of microwave antennas, components and subsystems based

on SIW technology," *IEEE MAPE,* vol. 1, pp.14-17, Aug. 2005.

[58] J. Hirokawa, and M. Ando, "Efficiency of 76-GHz post-wall waveguide-fed parallel-plate slot arrays," *IEEE Trans. Antennas Propagat.,* vol. 48, pp.1742-1745, Nov. 2000.

[59] H. Li, W. Hong, T-J Cui, K. Wu, Y. L. Zhang, and L. Yan, "Propagation characteristics of substrate integrated waveguide based on LTCC," *IEEE MTT-S,* vol. 3, pp. 2045-2048, Jun. 2003.

[60] Y. Huang, "Current distribution along a probe in a waveguide," *Ant. & Prop. SIS,* vol. 1, pp. 513-516, May 1990.

[61] H. Kai, J. Hirokawa, and M. Ando, "Analysis of the internal scattering field distribution in an oversized rectangular slotted waveguide," *IEEE Ant. & Prop. SIS,* vol. 2, pp. 250-253, Jul. 2001.

[62] K.W. Brown, "Design of waveguide slotted arrays using commercially available finite element analysis software," *Anten. & Propag. SIS,* vol. 2, pp. 1000-1003, Jul. 1996.

[63] D.R. Jahagirdar, "Effects of tolerances on sidelobe levels in slotted waveguide arrays," *IEEE Anten. & Propag. SIS,* vol. 3 pp. 3277-3280, Jun. 2004.

[64] J.Y. Li, and L.W. Li, "Smaller offset broadwall longitudinal waveguide slots: a new analysis using a new idea," *IEE Proc. Microw. Antenn. & Propag.,* vol. 152, no. 3, pp. 179-182, Jun. 2005.